Article

Experimental and Numerical Optimization Study on Performance of Solar Phase Change Thermal Energy Storage System

Yuqing Tang, Neng Zhu *, Siqi Li and Yingzhen Hou

School of Environmental Science and Engineering, Tianjin University, Tianjin, 300350, China; tangyq01_@tju.edu.cn
* Correspondence: nzhu@tju.edu.cn

Abstract: Promoting the use of solar energy resources has always faced the challenges of instability and supply-demand mismatch. The key to solving these issues is to efficiently store and utilize solar energy resources using high-performance heat storage devices. This study designed a high-performance shell-and-tube phase change thermal storage device and established a numerical model using ANSYS software to summarize the device's dynamic melting law. To verify the accuracy of the numerical simulation, a performance testing platform for the phase change thermal storage device was built to investigate the impact of factors such as inlet water temperature, inlet water flow rate, type of heat storage, and initial temperature of the device, and to reveal the change law of the device's performance. The results show that the inlet water temperature has the most significant impact on the device's heat storage and release performance. When the device's heat storage or release is used for heating, changing the inlet water flow rate has a weak and limited effect on the device's performance. However, when the device's heat release is used to provide domestic hot water, increasing the makeup water temperature and reducing the inlet water flow rate can significantly improve the device's effective heat release. Furthermore, based on the experimental validation of the model's correctness, this study further simulated and studied the impact of different factors on the device's heat storage process to optimize its structural design and provide technical references for the device's actual operation and installation. The results show that the placement of fins has a negligible effect on the performance of the heat storage device while reducing the fin spacing and increasing the fin thickness can significantly improve the melting efficiency of the phase change material (PCM). Additionally, the heat storage characteristics of the device are significantly better in the vertical installation mode than in the horizontal installation mode. This study provides theoretical guidance and technical references for the design and use of phase change thermal storage devices.

Keywords: phase change thermal energy storage device; solar energy; heat storage and release performance; experimental study; numerical simulation

1. Introduction

Solar energy boasts rich reserves, wide distribution, and a high degree of environmental friendliness. In China, over two-thirds of the country's regions receive annual radiation exceeding 5020MJ/㎡, while numerous winter heating areas possess considerable solar energy resources, providing an optimal basis for promoting the utilization of solar energy[1, 2]. However, despite the potential for replacing conventional energy sources with solar energy to reduce building heating energy consumption and carbon emissions, solar energy utilization still encounters stability issues. Furthermore, the supply of solar energy utilization systems conflicts with the building environment's construction load. This conflict is mainly due to the mismatch between the peak periods of solar energy supply and the trough periods of building heat load, and vice versa. Therefore, the development of high-performance and reliable heat storage equipment that can efficiently store and allocate solar energy resources is a crucial solution to address this problem.

Traditional heat storage tanks use water as the storage medium, which takes up large space, has low heat storage density, and suffers from severe heat loss. Compared with sensible heat storage, PCMs have higher heat storage capacity per unit volume, a stable temperature during melting or solidification phases, and can absorb or release large amounts of latent heat. Using PCMs as the

storage medium can downsize the equipment and facilitate the stable operation of the system. However, most PCMs have poor thermal conductivity, which reduces heat transfer efficiency and affects device performance. Therefore, optimizing the design of phase change thermal storage devices and exploring the performance variation rules have certain research significance.

Based on whether the fluid is in contact with the phase-change material, phase-change heat storage devices can be divided into direct contact and indirect contact types. The use of direct contact devices is complex and rare in practical applications. Indirect contact phase change thermal storage devices encapsulate the PCM through heat exchangers, making the operation more convenient and avoiding the loss of PCMs. PCMs are often encapsulated in rectangular containers, slender coils, and cylindrical containers. According to their packaging forms, indirect contact phase change thermal storage devices are mainly divided into three structures: plate, stacked, and tube-shell.

The structure of a flat-plate phase change TES system is relatively simple, and the plate size is a crucial factor affecting its performance. Many researchers have explored this issue. Prieto[3] et al. investigated the relationship between the thickness of the phase change plate and heat transfer efficiency, finding that reducing the thickness can enhance the heat transfer effect, increasing the heat transfer rate up to five times. Stacked TES systems are filled with encapsulated small-volume PCMs, and the heat transfer fluid flows through the gaps in the PCM stack, providing a larger heat transfer area than other methods. Reda[4] studied the effects of different diameters on the heat storage process of a stacked TES system with spherical encapsulation, finding that smaller diameter phase change spheres have relatively high heat transfer efficiency. Shamsi[5] et al. simulated the heat storage process of a stacked bed TES system and found that increasing the temperature or flow rate of the heat transfer fluid can improve the heat storage rate and amount. Compared with other methods, the shell-and-tube type TES system has a higher heat storage density per unit volume, simpler encapsulation of the PCM, and is easier to combine with various forms of heat exchangers, making it a preferred choice for over 70% of latent heat TES (LHTES) systems[6]. Vyshak[7] et al. studied the total time required for PCM to melt in containers with three different geometric configurations (rectangular, cylindrical, and cylindrical shell) with the same volume and heat transfer surface area, finding that cylindrical shells require the shortest time for equal energy storage under the same PCM mass and heat transfer surface area, and this geometric effect becomes more pronounced as the PCM mass increases. The common shell-and-tube heat transfer components are coil and jacket types. Coil types can achieve longer heat transfer paths in small sizes, effectively increasing the heat transfer time between the fluid and PCM, thereby improving heat transfer efficiency[8]. Liang[9] et al. simulated the effect of different pipe length-to-diameter ratios and PCM volume ratios on the performance of a shell-and-tube type phase change TES system, finding that effective energy storage ratio increases with an increase in the pipe length-to-diameter ratio and that there is an optimal PCM volume ratio. Only when the PCM volume ratio is greater than a certain value can an increase in the effective thermal conductivity of the PCM effectively improve the effective energy storage ratio.

Increasing the heat transfer area between the heat transfer fluid and PCM is an effective means of enhancing heat transfer efficiency, and attaching fins is a common way to increase the heat transfer area. Numerous studies have shown that the thermal performance of phase change thermal storage devices can be significantly improved by adding fins. Tay[10] et al. attached fins and pin fins to the heat transfer tube to enhance heat transfer efficiency in the intensification device and compared the improvement effects of the two through numerical simulation and experimental research. The results showed that the heat storage effect of fins was better, and the heat storage time was shortened by 25% compared with pin fins. Rathod[11] et al. conducted a comparative study on the heat storage performance of the phase change thermal storage device before and after the addition of fins. The results showed that the heat storage efficiency was significantly improved after adding three longitudinal fins. When the inlet temperatures of the heat transfer fluid were 80°C and 85°C, the heat storage time was shortened by 12.5% and 24.52%, respectively. Mat[12] et al. studied the inner fins, outer fins, and inner and outer fins enhancement technologies in the triplex-tube heat exchanger (TTHX), as well as the influence of fin length on the enhancement technology. The results showed that the three enhancement technologies did not have a significant difference in the PCM melting

 doi:10.20944/preprints202304.0481.v1

rate. Compared with the three-tube heat exchanger without fins, the time for complete melting of the inner and outer fins with a length of 42 mm was reduced by 43.3%.

The number, thickness, shape, and arrangement of fins have an impact on the performance of phase change TES systems. Al-Abidi[13] et al. numerically simulated the melting heat transfer process of PCM with fins inside and outside of a triple-tube heat exchanger (TTHX) and found that the melting time was influenced by the number of fins, the length of fins, and the thickness of fins. The complete melting times for 4, 6, and 8 fins were 69.5%, 56.5%, and 43.4%, respectively, compared to no fins. The melting times for fins with lengths of 10 mm, 20 mm, 30 mm, and 42 mm were 73.9%, 60.8%, 47.8%, and 43.4%, respectively, compared to no fins. The melting times for fins with thicknesses of 1 mm, 2 mm, 3 mm, and 4 mm were 43.4%, 39%, 39%, and 35%, respectively, compared to no fins. Yuan[14] et al. simulated a cylindrical phase change TES unit using paraffin RT82 as the PCM and established different numerical models by changing the number and width of fins and the radius of the cylindrical TES tube to compare their TES performance and obtain optimal model parameters. Castell[15] et al. conducted experimental research on a phase change TES system with fins and pointed out that the melting rate increased with the decrease of fin spacing and the increase of the temperature difference between the heat transfer fluid and the PCM. Shatikian[16] et al. studied the effect of different fin thicknesses on the TES process of a phase change TES system, and found that increasing the fin thickness accelerated the melting of the PCM, but shortened the fin spacing and reduced the amount of PCM. A reasonable configuration of fin thickness and spacing can improve the heat transfer performance of the TES system.

Alvaro[17] et al. conducted a comparative study between a pure water TES system and a plate heat storage system using paraffin as a PCM. The results showed that the volume of the phase change heat storage system was half that of the pure water system when storing the same amount of heat, and it had better heat storage and release capacity. Prieto[18] et al. investigated the effect of different PCMs on the heat storage and release performance of the same structure, and the results showed that paraffin with higher enthalpy had stronger heat storage capacity and longer heat release duration, while stearic acid with higher heat transfer coefficient had better heat transfer effect and could better meet the load demand during peak hours. Bansal[19] et al. used organic acid as the phase change heat storage material and verified the applicability of the heat transfer model combining solar collectors and phase change heat storage under various operating conditions using numerical simulation. The results showed that the system combining PCMs and collectors was superior to the system separating PCMs and collectors. Rathod[20] et al. used the AHP method combined with TOPSIS and fuzzy TOPSIS methods to select the optimal PCM for a solar hot water system. Xu[21] et al. used the AHP and TOPSIS methods to select the optimal PCM for a solar air conditioning system and validated the selected results through Ashby's method.

Al-Abidi[22] et al. investigated the application of a three-tube heat exchanger in a liquid desiccant air conditioning system, studying three different processes: inner tube heating, outer tube heating, and double-side tube heating, and analyzing the temperature gradients of PCM in radial, angular, and axial directions. The results showed that double-side tube heating could achieve complete PCM melting in a shorter time and at a lower inlet temperature. Hosseini[23] et al. conducted experimental research and simulation analysis on a horizontally positioned shell-and-tube latent heat storage unit, showing that raising the temperature of the heat transfer fluid can shorten the melting time of the PCM, and the melting time of the PCM was reduced by 37% when the inlet water temperature was 80°C. Rathod[24] et al. conducted experimental research on the vertical shell-and-tube unit during the heat storage process, changing the inlet flow rate and the temperature of the heat transfer fluid to observe the melting differences in the unit. The results showed that reducing the mass flow rate or inlet temperature of the heat transfer fluid would increase the total melting time of the PCM, and the effect of the fluid inlet temperature on the melting of the unit during the PCM melting process was more significant than the mass flow rate. Wang[25] et al. simulated the heat storage performance of a shell-and-tube phase change heat storage unit, showing that increasing the inlet flow rate of the heat transfer fluid would decrease the total energy efficiency ratio of the unit

 doi:10.20944/preprints202304.0481.v1

while increasing the heat storage rate and raising the inlet temperature of the heat transfer fluid could simultaneously improve the heat storage rate and energy efficiency ratio of the unit.

The design and enhancement of heat exchange in phase change thermal storage devices can be summarized as follows: (1) Compared to direct and indirect contact-type phase change thermal storage devices, the tube-and-shell structure has advantages such as versatility in combination with various heat exchangers, convenient packaging, and high heat storage density, making it more favored by researchers. (2) The performance of phase change thermal storage devices is affected by factors such as the number, thickness, spacing, shape, and arrangement of fins. (3) The heat storage effect of phase change thermal storage devices is influenced by factors such as the inlet temperature and flow rate of the heat exchange fluid, and flow direction.

There are still several issues in the current research on phase change thermal storage devices: (1) Regarding device design, the function of phase change thermal storage devices is relatively single, mostly used for indoor heating or providing hot water for residential use during winter. Most studies use expensive copper as the heat exchange component in the device, which poses difficulties for household use or large-scale production. (2) In terms of numerical simulation, the heat exchange tube is often simplified as a partial tube section, and the heat storage and release process is simulated and analyzed. However, the numerical model is significantly different from the actual structure. For example, for longer coiled pipes, the temperature of the heat exchange fluid changes during flow, resulting in discrepancies between the results obtained from analyzing partial pipe sections and the actual performance. (3) In terms of operating conditions, most studies focus on the effects of heat exchange fluid temperature and flow rate on the heat storage performance of the device and the effects of heat exchange fluid flow rate and initial device temperature on the heat release performance of the device. Research on the effects of heat exchange fluid flow direction on the heat storage performance of the device and the effects of heat exchange fluid temperature on the heat release performance of the device is limited. (4) In terms of performance analysis, some studies only evaluate the performance of the device based on the melting or solidification effect of the PCM, without considering the heat storage capacity, instantaneous power, and effective heat release efficiency of the device under different operating conditions.

This paper has mainly accomplished the following tasks: (1) Development of a phase change thermal energy storage device with a small footprint, high energy storage density, and excellent thermal storage and release performance. The device can effectively balance the energy supply and demand in buildings, and in combination with the design of electric heating plates, it is conducive to the comprehensive utilization of renewable energy, making it an efficient and stable solar thermal storage technology. (2) The experimental and numerical simulation methods were combined to verify the reliability of the numerical simulation through experiments. The effects of various factors on the thermal storage and release performance of the phase change thermal energy storage device were studied. The influence of the fin structure of the device on its performance was also investigated through simulation.

The structure of this paper is as follows: Section 2 introduces the physical model, control equations, and numerical simulation methods. Section 3 describes the phase change experiments. Section 4 summarizes and analyzes the experimental results. Section 5 uses numerical simulation methods to study the performance of the phase change thermal storage device.

2. Materials and Method

2.1. Physical model

The physical model diagram of the phase change TES device studied in this paper is shown in Figure 1. The physical model of the device mainly consists of a metal coil with fins and a square box outside the device. The internal space of the box is 820 mm long, 290 mm wide, and 800 mm high. There is one group of serpentines with fins inside the box, and each group of coils is composed of 10 straight pipes with a length of 700 mm, 9 semicircular pipes with a radius of 38 mm, and inlet and

Preprints (www.preprints.org) | NOT PEER-REVIEWED | Posted: 18 April 2023 doi:10.20944/preprints202304.0481.v1

outlet pipes. The fin thickness is 1 mm, and the fin spacing is 50 mm. The heat transfer fluid enters from the top of the coil and exits from the bottom.

Due to the extremely complex phase change process, the heat storage calculation process of the device is simplified by the following assumptions to reduce the computation time:

(1) The outer wall of the device box has good insulation properties, and the heat loss of the phase change device is ignored.

(2) The PCM is isotropic, and the physical parameters of the solid and liquid phases are constant and do not change with temperature.

(3) Natural convection heat transfer between liquid PCMs is considered by introducing the *Boussinesq* assumption.

(4) The heat transfer fluid is an incompressible Newtonian fluid.

(5) Axial heat conduction and viscous dissipation in the heat transfer fluid are neglected.

(6) Since the flow and heat transfer of water in the finned tube are axisymmetric, the phase change device can be simplified to a two-dimensional model.

2.2. Control equation

Based on the above assumptions, a transient two-dimensional control equation is established to describe the phase-change region. The continuity equation is used to describe the law of density change of the fluid, which states that the net mass inflow into a certain control volume per unit of time is equal to the increase in mass of the control volume during that time. In a Cartesian coordinate system, its differential form is as follows:

$$\frac{\partial \rho}{\partial \tau}+\frac{\partial(\rho u)}{\partial x}+\frac{\partial(\rho v)}{\partial y}=0 \tag{1}$$

Here, ρ represents fluid density, τ denotes time in seconds (s), u represents the x-component of the velocity vector in meters per second (m/s), and v represents the y-component of the velocity vector in meters per second (m/s).

$$\frac{\partial u}{\partial x}+\frac{\partial v}{\partial y}=0 \tag{2}$$

The momentum conservation equation is used to describe the momentum equation of viscous incompressible fluids, which states that the rate of change of the total momentum of a control volume microelement in a unit of time is equal to the sum of all external forces acting on the microelement control volume during that time. In the Cartesian coordinate system, its differential form is expressed as:

$$\rho\left(\frac{\partial u}{\partial \tau}+u\frac{\partial u}{\partial x}+v\frac{\partial u}{\partial y}\right)=f_x+\mu\left(\frac{\partial^2 u}{\partial x^2}+\frac{\partial^2 u}{\partial y^2}\right)-\frac{\partial P}{\partial x} \tag{3}$$

$$\rho\left(\frac{\partial v}{\partial \tau}+u\frac{\partial v}{\partial x}+v\frac{\partial v}{\partial y}\right)=f_y+\mu\left(\frac{\partial^2 v}{\partial x^2}+\frac{\partial^2 v}{\partial y^2}\right)-\frac{\partial P}{\partial y} \tag{4}$$

Here, f_x and f_y represent the components of the volume force in the x and y directions, respectively, in units of Pa; μ represents the dynamic viscosity coefficient in units of N·s/m2; P represents the pressure, in units of Pa.

The energy equation is the differential form of the first law of thermodynamics, which is a fundamental equation for analyzing flow systems with heat exchange. It describes the rate of change of the total energy of a control volume element over a unit of time, equal to the sum of the net rates of energy transfer in and out of the element, and the work done on the element by surface and body forces. In rectangular coordinates, its differential form is expressed as follows:

$$\frac{\partial(\rho T)}{\partial \tau}+div(\rho\vec{v}T)=div\left(\frac{\lambda}{C_P}grandT\right)+S_T \tag{5}$$

Here, T denotes the temperature in Kelvin (K), λ represents the thermal conductivity of the fluid in units of W/(m·K), C_P is the specific heat capacity at constant pressure in units of J/(kg·K), and S_T stands for the source term.

The governing equations for the enthalpy-based model in this study are given as follows:

$$\frac{d}{dt}\int_V \rho h dV+\int_S \rho h dA=\int_S \lambda \nabla T dA+\int_V q dV \tag{6}$$

Preprints (www.preprints.org) | NOT PEER-REVIEWED | Posted: 18 April 2023 doi:10.20944/preprints202304.0481.v1

Here, $\boldsymbol{h}$ represents the enthalpy of PCM in kJ/kg, $\boldsymbol{\rho}$ represents the density of PCM in kg/m3, and $\boldsymbol{\lambda}$ represents the thermal conductivity of PCM in W/(m·K).

When the specific heat of the solid-liquid phase of the PCM is constant, the relationship between temperature and enthalpy is as follows:

$$\boldsymbol{h = h_s + L} \tag{8}$$

$$\boldsymbol{h = h_{ref} + \int_{T_{ref}}^{T} C_P dT} \tag{9}$$

Here, $\boldsymbol{L}$ represents the latent heat of the phase-change material, measured in kJ/kg, $\boldsymbol{T_{ref}}$ represents the reference temperature, measured in K, and $\boldsymbol{h_{ref}}$ represents the enthalpy of the phase-change material at the reference temperature, measured in kJ/kg.

2.3 Numerical simulation

A 2D model of a phase change TES device was established using DesignModeler in ANSYS Workbench software for simulation. The model was then imported into the Meshing module for grid generation. The grid quality evaluation needed to consider the calculation time and accuracy of the numerical simulation. Therefore, a mesh independence test was performed to compare the simulation results of different mesh quantities. Considering both the calculation accuracy and speed, a mesh model with a quantity of 32118 was selected as shown in Figure 3. The model was then imported into the FLUENT software for simulation, which is based on enthalpy-porosity and finite volume methods.

$$\beta = \begin{cases} 0, & T \le T_s \\ \dfrac{T - T_s}{T_l - T_s}, & T_s < T < T_l \\ 1, & T \ge T_l \end{cases} \tag{10}$$

$\boldsymbol{T_s}$ represents the solid phase line temperature of the PCM, expressed in Kelvin (K). $\boldsymbol{T_l}$ represents the liquid phase line temperature of the PCM, expressed in Kelvin (K).

The energy storage performance of the phase change TES system determines the amount of usable energy during the night. The evaluation indicators for the energy storage process mainly include the inlet and outlet water temperature difference, the total amount of stored heat, and the average stored heat power.

$$Q_x = \frac{\int_{t_1}^{t_2} \rho c_p V (T_{in} - T_{out}) dt}{3600} \tag{11}$$

$$\overline{P_x} = \frac{Q_x}{t_2 - t_1} \tag{12}$$

Here, $\boldsymbol{Q_x}$ represents the stored heat capacity of the device in kJ, $\boldsymbol{\overline{P_x}}$ represents the average stored heat power in kW, $\boldsymbol{t_1}$ is the start time of the energy storage process in seconds, $\boldsymbol{t_2}$ is the end time of the energy storage process in seconds, ϱ is the density of water in kg/m³ (assumed as 1000 kg/m³), $\boldsymbol{c_p}$ is the specific heat capacity of water at constant pressure in kJ/(kg·K) (taken as 4.2 kJ/(kg·K)), V is the flow rate of the inlet water in m³/h, $\boldsymbol{T_{in}}$ is the inlet temperature of the device in ℃, and $\boldsymbol{T_{out}}$ is the outlet temperature of the device in ℃.

The heat release performance of the phase change TES system determines the energy utilization efficiency on the demand side. The evaluation indicators for the heat release process mainly include the inlet and outlet water temperature difference, effective heat release time, effective heat release efficiency, and heat release power. Among them, the effective heat release efficiency is defined as the ratio of the energy content in the water discharged from the TES during the effective heat release time to the stored heat energy in the TES at the beginning of the heat release process.

$$Q_s = \frac{\int_{t_1}^{t_2} \rho c_p V (T_{out} - T_{in}) dt}{3600} \tag{13}$$

Preprints (www.preprints.org) | NOT PEER-REVIEWED | Posted: 18 April 2023 doi:10.20944/preprints202304.0481.v1

$$\eta = \frac{Q_s}{Q_x} \tag{14}$$

Here, $\boldsymbol{Q_s}$ represents the heat released by the device, measured in kJ; $\boldsymbol{\eta}$ denotes the effective energy release efficiency; $\boldsymbol{t_1}$ and $\boldsymbol{t_2}$ represent the start and end times of the heat release process, measured in seconds.

The formula for calculating the instantaneous heat release power is as follows:

$$P = \frac{\rho c_p V (T_{out} - T_{in})}{3600} \tag{15}$$

The Heat release conditions considered in this paper are classified into two types: effective heat release occurs when the device releases heat for heating and its heat release power is higher than the building heat load (P≥0.338kW). According to the Building Water Supply and Drainage Design Code GB50015-2019, the recommended water temperature for shower use is 37~40℃, while for washbasin spout uses it is 30℃. Additionally, the maximum daily water consumption quota per person per day is 400~480L. Therefore, when the device releases heat for a domestic hot water supply, an outlet water temperature higher than 37°C ($\boldsymbol{T_{out}}$≥37°C) is considered effective for showering and domestic hot water an outlet water temperature higher than 30°C ($\boldsymbol{T_{out}}$≥30°C) is considered effective. This paper particularly emphasizes the heat release of the device when the outlet water temperature exceeds 37°C.

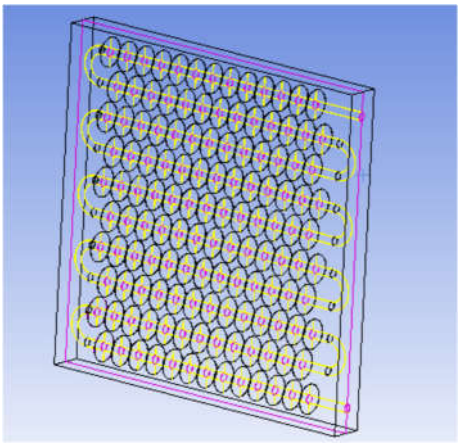

Figure 1. Physical model of the phase change heat storage system.

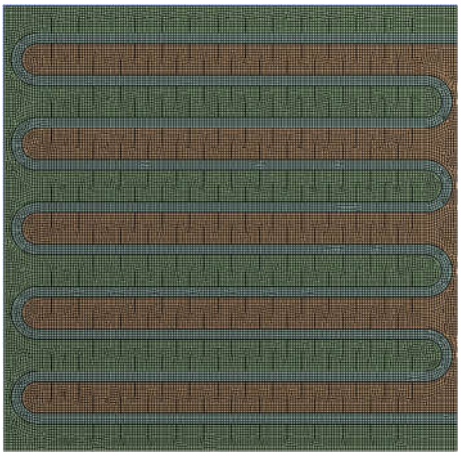

Figure 2. A mesh model of phase change TES system.

Preprints (www.preprints.org) | NOT PEER-REVIEWED | Posted: 18 April 2023 doi:10.20944/preprints202304.0481.v1

3. Experimental verification

3.1. Experimental purpose and principle

The purpose of building a performance testing experimental platform for the latent heat storage device is twofold: firstly, to verify the accuracy of numerical simulation and lay a foundation for the optimization of phase-change heat storage devices through simulation research; secondly, to investigate the effects of different factors such as inlet water temperature, inlet flow rate, heat storage, and release mode, and initial temperature on the device's heat storage and release performance. This aims to explore the influencing factors of the device's heat storage and release performance and provide references for the practical application of phase-change heat storage devices. Due to limitations in the experimental site and conditions, an electric boiler was used to simulate the solar collector outlet water and user heating return water, and a chiller was used to simulate the cold water replenishment for domestic hot water. As shown in Figure 1, a performance-testing experimental platform for phase-change heat storage devices was built to conduct experiments on the heat storage and release performance of the device.

The experimental system principle is illustrated in Figure 4. During the charging process, hot water flows from the electric boiler into the phase-change heat storage device for heat exchange, passes through the water pump, and then returns to the electric boiler for reheating. During the discharging process, the electric boiler or the chiller provides low-temperature water at a specified temperature, which flows into the phase-change heat storage device to absorb heat and raise the water temperature. The temperatures at different measurement points within the device and the inlet and outlet water temperatures are recorded under different conditions using a data logger.

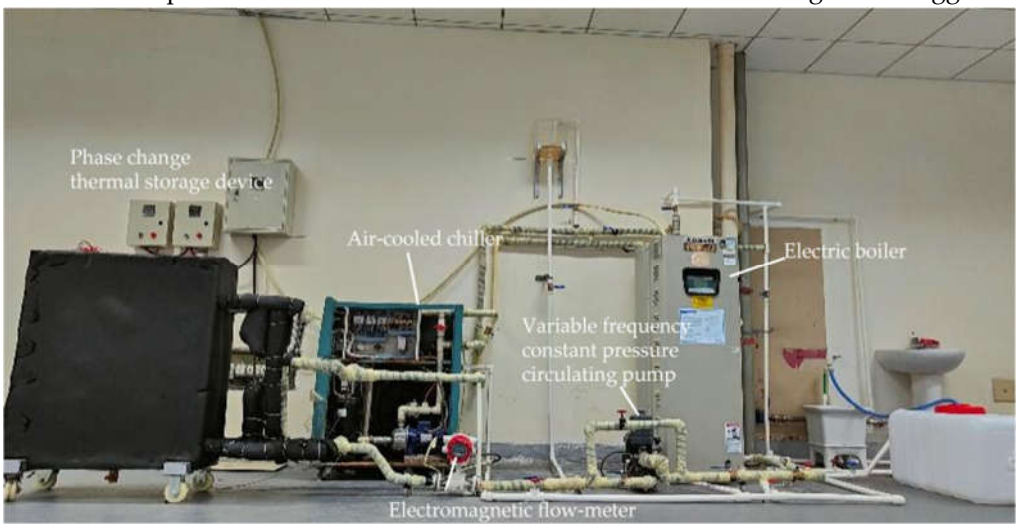

Figure 3. Experimental setup for testing the performance of the phase change TES device.

Preprints (www.preprints.org) | NOT PEER-REVIEWED | Posted: 18 April 2023 doi:10.20944/preprints202304.0481.v1

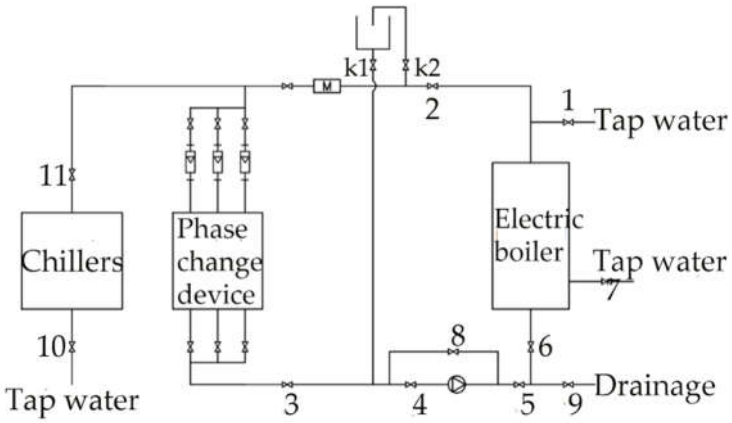

Figure 4. Schematic of the experimental system.

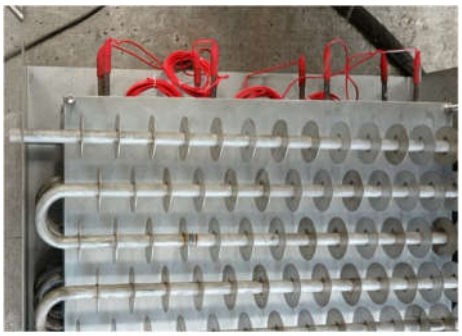

Figure 5. The real structure of phase change TES device.

Preprints (www.preprints.org) | NOT PEER-REVIEWED | Posted: 18 April 2023 doi:10.20944/preprints202304.0481.v1

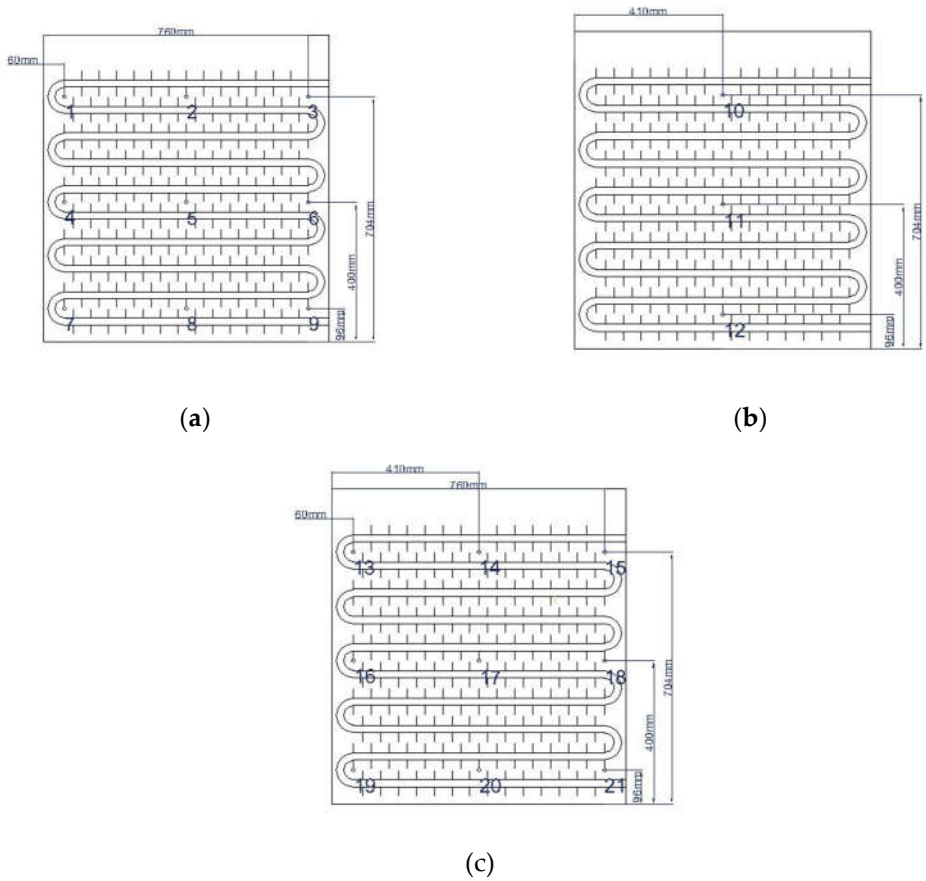

(a) (b)

(c)

Figure 6. Diagram of temperature measurement points layout inside the phase change thermal storage device: (a) Tube coil 1; (b) Tube coil 2; (c) Tube coil 3

3.2. Experimental apparatus

The internal structure of the phase change device is shown in Figure 5, consisting of a heat storage box, finned coils, and electric heating plates with the main parameters listed in Table 1. The equipment used in the experiment and their technical specifications are detailed in Table 2. During the charging process, hot water exchanges heat with the PCM as it flows through the device, and then is reheated in the electric boiler after passing through a pump. During discharging, low-temperature water from the electric boiler or chiller enters the device, absorbs the heat released by the PCM, and then exits at a higher temperature. The temperature of PCM inside the device can reflect the process of heat storage and release in the phase change device, while the temperature difference between the inlet and outlet of the device can reflect the heat storage and release effect of the phase change device. Therefore, the focus of this experiment is to measure the temperature of the PCM inside the device and the inlet and outlet water temperatures of the device. As the water flows into the device from the top and exits from the bottom, there are temperature differences at different heights inside the device, and the structure at different positions in the same horizontal direction is not identical, resulting in different heat transfer effects. Therefore, measurement points are arranged at different positions inside the device to detect temperature changes. The specific arrangement of the measuring points is shown in Figure 6. Temperatures at different points inside and the inlet and outlet of the device are recorded by a data acquisition system consisting of K-type thermocouples, a data logger, and MX-100 Standard software on a PC. The temperature readings are displayed and recorded in real-time by the software.

Preprints (www.preprints.org) | NOT PEER-REVIEWED | Posted: 18 April 2023 doi:10.20944/preprints202304.0481.v1

Table 1. Detailed parameters of the main components inside the phase change TES device.

Name	Material	Relevant parameters
heat storage tank	304 stainless steel	Internal Dimensions: 820×320×800mm Wall Thickness: 2mm Diameter：18mm External Diameter: 20mm
Finned tube coil	304 stainless steel	Vertical center distance between adjacent coils: 304mm Horizontal center distance between adjacent coils: 80mm Distance to the bottom wall of the box: 25mm Distance to the top wall: 128mm
Electric heating plate	Aluminium	Dimensions: 700×25×800mm Distance to the top wall surface: 80mm

Table 2. The main equipment and instrument parameters of the experiment.

Name	Manufacturer source	Model	Relevant parameters
Electric boiler	A.O. Smith	DSE-50-90	Heating power: 18 kW Temperature control range for water: 30~88℃ Rated capacity: 190 L Minimum differential temperature: 1℃
Air-cooled chiller	Zhongke Kechuangyi	KYKY-LS 65A	Cooling capacity: 6.5kW Water temperature control range: 10~25 ℃ Water tank capacity: 40L Water control accuracy: ±0.2℃
Variable frequency constant pressure circulating pump	Grundfos	CM5-3	Rated power: 650W Max. variable flow rate: 4.7m3/h
Electromagnetic flowmeter	Meikon	LDG-SUP-DN10	Measurement range: 0~1.4m³/h Accuracy class: ±0.5%R
Rotor flowmeter	Juyi Instrument	LZB-WS-10G	Measurement range: 16~160L/h
Thermocouple	Xiamen Mingkong	K-type	Length: 2.5m
Data logger	Yokogawa	MX-100	Inputs for DVC/TC/DI/RTD

3.3. PCM

The present study focuses on the application of a PCM (PCM) in a solar thermal system for providing space heating and domestic hot water in residential buildings. To meet the operational requirements of the system, a commercially available PCM produced by Hubei Saimo New Energy Technology Co., Ltd. in China with a phase change temperature range of 45–50 °C is selected. The PCM exhibits high energy storage density, small undercooling, and good thermal stability, as evidenced by differential scanning calorimetry (DSC) testing. The melting onset, peak, and end temperatures are 46.1, 50.5, and 52.7 °C, respectively, with a melting enthalpy of 238.2 kJ/kg, while the solidification onset, peak, and end temperatures are 36.9, 44.8, and 48.1 °C, respectively, with a solidification enthalpy of 236.9 kJ/kg.

Preprints (www.preprints.org) | NOT PEER-REVIEWED | Posted: 18 April 2023 doi:10.20944/preprints202304.0481.v1

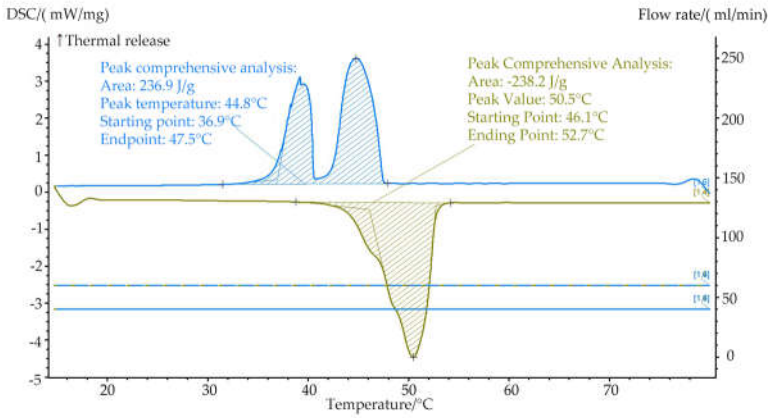

Figure 7. DSC performance test curve of PCM TH-SL49.

3.4. Experimental design

To investigate the effects of inlet temperature, inlet flow rate, and device temperature on the heat storage and release performance of the device, this experiment set different operating condition parameters for the heat storage, heating release, and domestic hot water release, and the specific schemes are shown in Table 4 and Table 5.

Table 4. Heat storage test conditions.

Number	The initial temperature of the device (℃)	Inlet water temperature (℃)	Inlet water flow rate (m³/h)	Heat storage mode
1	33	58	0.27	Hot water
2	33	63	0.27	Hot water
3	33	68	0.27	Hot water
4	33	68	0.18	Hot water
5	33	68	0.36	Electric heating plate + Hot water
6	33	68	0.36	Hot water

Table 5. heat release test conditions.

Number	Number	The initial temperature of the device (℃)	Inlet water temperature (℃)	Inlet water flow rate (m³/h)
Heating release condition	7	63	25	0.27
	8	63	30	0.27
	9	63	35	0.27
	10	63	30	0.18
	11	63	30	0.36
	12	53	30	0.27
	13	58	30	0.27
Domestic hot water release condition	14	58	25	0.05
	15	58	25	0.08
	16	58	25	0.11
	17	58	30	0.08

Preprints (www.preprints.org) | NOT PEER-REVIEWED | Posted: 18 April 2023 doi:10.20944/preprints202304.0481.v1

4. Results and discussion

4.1. Numerical simulation and experimental results comparison and validation

To verify the consistency between the experimental and simulation results, Figure 10 compares the measured and simulated temperatures at measurement points 13 and 17 under two heat storage conditions. As shown in the figure, the simulated values of both measurement points are consistent with the experimental values under the same thermal storage condition. However, due to the simplification assumption and neglect of heat loss in the phase change device during numerical simulation, there is a deviation between the simulated and measured values. The average relative errors between the simulated and measured values of the two measurement points in heat storage process (a) are 2.69% and 6.24%, respectively, while those in thermal storage process (b) are 3.13% and 5.86%, respectively. Therefore, the consistency between the experimental and simulation results is good.

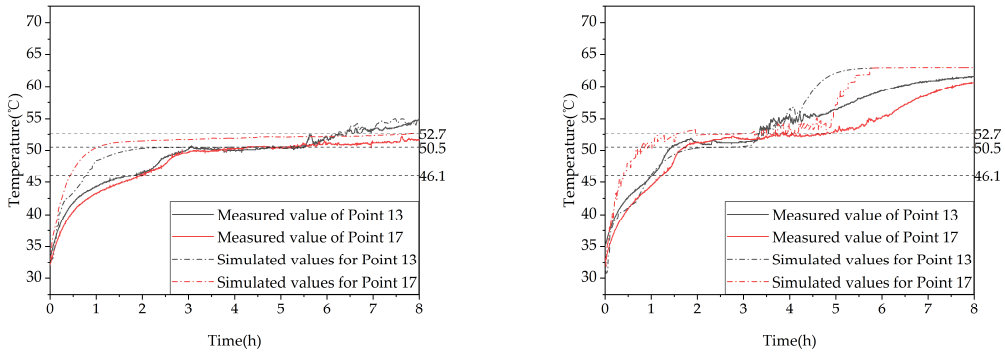

Figure 8. The temperature-time curves of simulated and experimental measurement points: (**a**) Inlet temperature of 58℃ and flow rate of 0.27 L/s; (**b**) Inlet temperature of 63℃ and flow rate of 0.27 L/s.

4.2. Heat storage and release characteristics of phase change thermal storage device

Figure 9(a) depicts the evolution of TES temperature at different positions within the apparatus. Three dashed lines indicate the beginning, peak, and end temperatures of the PCM (PCM) melting process. The figure demonstrates that the PCM TES process can be categorized into three distinct stages: (i) an initial stage, during which the PCM is in a sensible heat storage state and has not undergone any phase change; at this stage, the temperature rises relatively fast due to the large temperature difference between the inlet water and the PCM, and the heat transfer occurs mainly through conduction; (ii) a middle stage, during which the PCM undergoes a phase change and is in a latent heat storage state, resulting in a considerably reduced temperature rise rate; at this stage, PCM close to the tube wall and fins melts first due to the density difference, causing liquid PCM to rise and solid PCM to sink, resulting in natural convection as the predominant heat transfer mechanism; and (iii) a late stage, during which the PCM completes the phase change process and enters another sensible heat storage stage, resulting in a significantly increased temperature rise rate. As the temperature difference between the PCM and the inlet water is smaller during this stage, the heat transfer mechanism is mainly conduction, but the temperature rise rate is slower than that in the initial stage. Additionally, the temperature curves of some measuring points exhibit fluctuations at the end of melting and during the transition back to the initial sensible heat storage stage due to the coexistence of melted and solid PCM in the vicinity of these points, resulting in heat and mass transfer phenomena. Moreover, periodic fluctuations in the inlet water temperature caused by the 2°C hysteresis of the electric boiler can also cause fluctuations in the temperature measurements at the measuring points within the apparatus.

Figure 9 (b) depicts the variation in heating release temperature over time at measurement points within the apparatus. This trend comprises three distinct phases. In the initial heating release stage, the PCM remains in a sensible heating release state and does not undergo any phase change. During

 doi:10.20944/preprints202304.0481.v1

this stage, there exists a large temperature difference between the incoming water and the PCM, resulting in a rapid temperature rate decrease. The predominant heat transfer mechanism is convective heat transfer. In the middle heating release stage, the PCM reaches its solidification temperature and continues to release heat to the incoming cold water. The device is now in a latent heating release state, and the temperature rate decreases relatively smoothly. During this stage, the PCM close to the tube wall and fins undergoes solidification due to the density difference. The solidified PCM sinks under gravity, while the un-solidified liquid PCM rises due to its lower density. Consequently, the natural convection effect weakens gradually as the liquid phase in the apparatus decreases. In the later heating release stage, the PCM gradually completes the phase change process, concluding the latent heating release stage and re-entering the sensible heating release stage. The main heat transfer mechanism during this stage is thermal conduction.

Figure 9 (c) shows the trend of the heating release temperature at measurement points inside the device over time during the domestic heating process. Similar to the heating release process of the heating system, the domestic heating release process can also be divided into three stages: an initial heating release stage where the temperature drops rapidly and the PCM remains in a sensible heating release state, a middle heating release stage where the temperature drop rate decreases relatively smoothly and the PCM undergoes latent heating release and a later heating release stage where the temperature drop rate increases again and the PCM gradually completes the phase change process. Unlike the heating release process of the heating system, the temperature drop rate at each measuring point decreases as the incoming water flow rate increases, and the temperature at each measuring point decreases as the heating release process ends and more incoming water flows in.

The overall trend of TES temperature change in different coil groups is consistent, as shown in Figures 9(a)- 9(b). Among them, there are 6 representative lines, where measuring points 1 and 9 correspond to the most and least favorable heat transfer points of coil group 1, measuring point 11 is the center point of coil group 2, and also the center point of the phase change heat storage apparatus, and measuring points 13, 17, and 21 correspond to the most favorable, center, and least favorable heat transfer points of coil group 3, respectively. Therefore, representative measuring points are selected for comparison under different operating conditions in subsequent sections.

Comparing different operating conditions in the experiment, this study analyzes the influence of factors such as inlet temperature, inlet flow rate, and device temperature on the heat storage and release performance of the device.

Preprints (www.preprints.org) | NOT PEER-REVIEWED | Posted: 18 April 2023 doi:10.20944/preprints202304.0481.v1

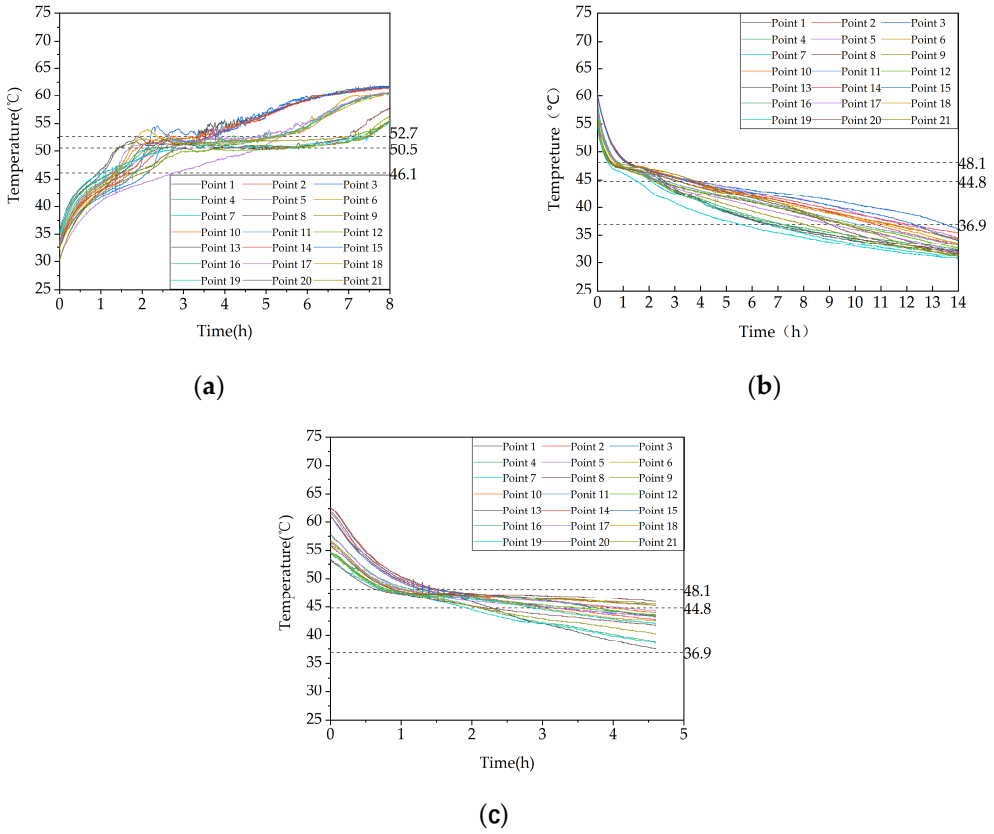

Figure 9. Temperature variation inside the phase change heat storage: (a) Heat storage condition (with the inlet water temperature of 63℃ and an inlet flow rate of 0.27 m³/h); (b) Heat release condition of heating (with the initial temperature of the device at 58℃, and the water inlet temperature and flow rate at 30℃ and 0.27m³/h, respectively; (c) Domestic hot water heat release condition (with the initial temperature of 58 ℃, an inlet water temperature of 25 ℃, and a flow rate of 0.05 m³/h).

4.3. Inlet temperature

4.3.1. Heat storage performance

To investigate the effect of storage temperature on the heat storage performance of a phase change thermal storage device, experiments were conducted under three different inflow temperatures of 58℃, 63℃, and 68℃ with a controlled inflow rate of 0.27m³/h, corresponding to test conditions 1-3 in Table 4. The temperature variations inside the device for the three storage conditions are shown in Figure 10. When the inflow temperature was increased from 58℃ to 63℃, the duration of the storage phase at measuring points 13, 17, and 21 decreased by 44%, 33.9%, and 30.4%, respectively. Similarly, when the inflow temperature was increased from 63℃ to 68℃, the duration of the storage phase at these points decreased by 24.6%, 29.7%, and 24.4%, respectively. When the inflow temperature was increased from 58℃ to 68℃, the duration of the storage phase at these points decreased by 57.8%, 53.6%, and 47.4%, respectively. Thus, increasing the inflow temperature can significantly enhance the storage performance, especially at lower storage temperatures.

Figure 11 shows the variation of the temperature difference between the inlet and outlet of the device with time at different inlet temperatures. As can be seen from the figure, at the beginning of the charging process, the temperature differences between the inlet and outlet of the three working conditions were 11.1℃, 7.4℃, and 19.7℃, respectively. At the end of the charging process, the temperature differences were reduced to 2.9℃, 1.8℃, and 1.2℃, respectively. Therefore, as the inlet temperature increases, the thermal storage performance of the device is improved, and more heat is stored in the phase change material, resulting in a gradual decrease in the temperature difference between the inlet and outlet. The total amount of heat stored corresponding to the three working

Preprints (www.preprints.org) | NOT PEER-REVIEWED | Posted: 18 April 2023 doi:10.20944/preprints202304.0481.v1

conditions were 32744kJ, 42393kJ, and 48002kJ, with average charging powers of 1.14kW, 1.47kW, and 1.67kW, respectively. When the inlet temperature was increased from 58℃ to 63℃, the amount of heat stored by the device increased by 29.47% or 46.60%, respectively.

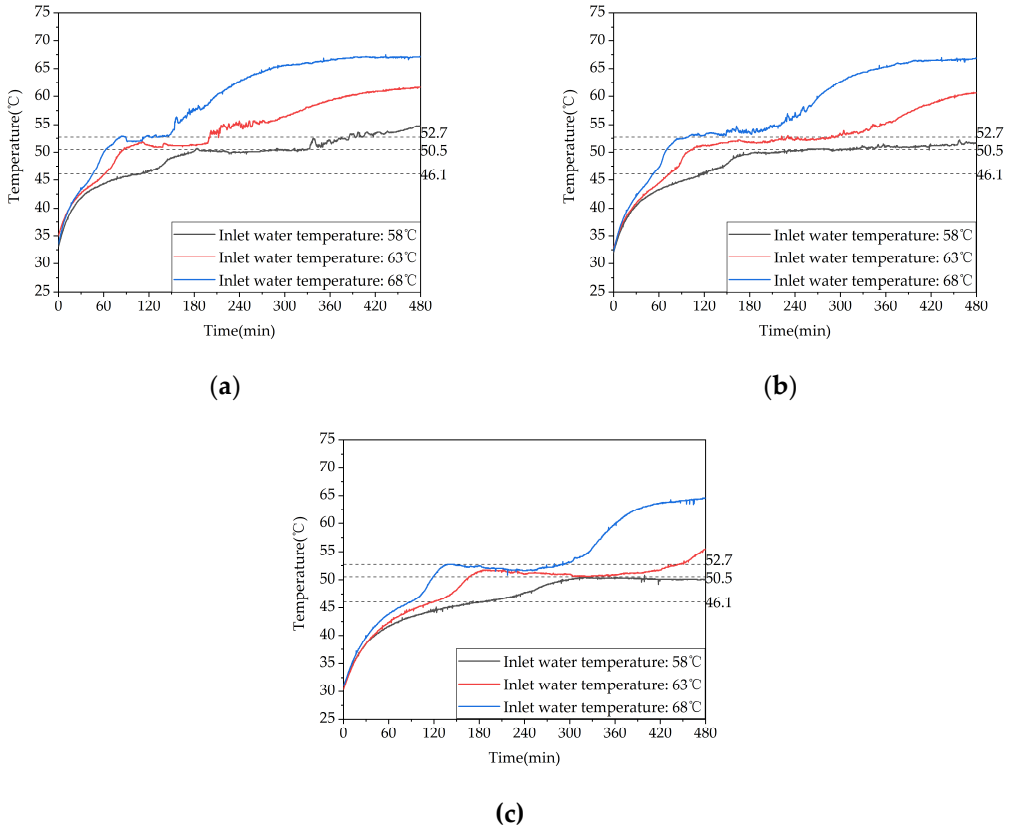

Figure 10. Temperature variation inside the phase change heat storage unit at typical locations under different Heat storage conditions: (a) Measuring point 13; (b) Measuring point 17; (c) Measuring point 21.

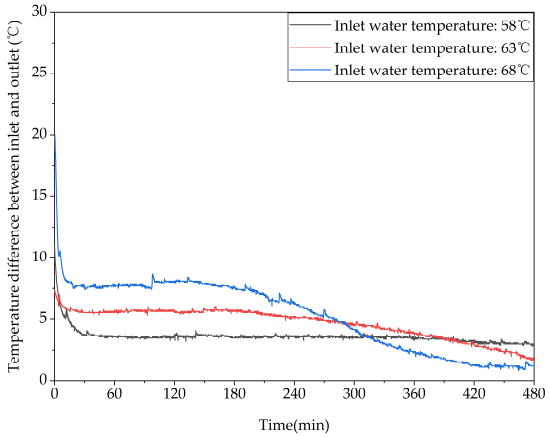

Figure 11. Different trends of the temperature difference between the inlet and outlet of the device over time under different inlet water temperatures.

4.3.2. Heat release performance of heating

To investigate the influence of inlet water temperature on the heating performance of phase change heating systems, heating performance tests were conducted under three different inlet water temperatures, namely, 25℃, 30℃, and 35℃, with a constant flow rate of 0.27 m³/h. The corresponding

 doi:10.20944/preprints202304.0481.v1

heating conditions are labeled as test conditions 7-9 in Table 5. The temperature changes inside the phase change device at different locations for the three storage heating conditions are shown in Figure 12. It can be seen from the figure that as the inlet water temperature increased from 25℃ to 30℃, the time taken for measurement points 13, 17, and 21 to reach the end of the heat release temperature was extended by 94.9%, 77.2%, and 46.1%, respectively. When the inlet water temperature was further increased from 30℃ to 35℃, the time taken for these measurement points to reach the end of the heat release temperature was extended by 46.6%, 21.2%, and 32.3%, respectively. When the inlet water temperature was increased from 25℃ to 35℃, the time taken for these measurement points to reach the end of the heat release temperature was 2.86 times, 2.15 times, and 1.93 times longer than the original time, respectively. Therefore, increasing the inlet water temperature can significantly prolong the heat release duration of the device. In addition, as the distance between the measurement points and the inlet of the thermal fluid increased, the start time of phase change gradually shortened due to the poorer heat transfer effect at measurement points that were farther away from the inlet during the heat storage phase. As a result, the time taken for these measurement points to reach the end of the heat release temperature gradually increased because increasing the inlet water temperature reduced the temperature difference between the PCM and the inlet water, thereby weakening the heat transfer effect.

Figure 13 shows the variations of the temperature difference at the inlet and outlet of the system and the instantaneous heat release rate as a function of time for different inlet water temperatures. As depicted in Figure 13(a), the temperature differences between the inlet and outlet at the end of the heat storage phase are 0.7 ℃, 1.0 ℃, and 1.0 ℃ for the inlet water temperatures of 25 ℃, 30 ℃, and 35 ℃, respectively. Moreover, Figure 13(b) illustrates that the instantaneous heat release rates at the initial stage of heat release exhibit significant differences among the three operating conditions, with higher inlet water temperatures leading to lower heat release rates. As the heat release process progresses, the heat release rates gradually decrease, and the differences among the three operating conditions become smaller. These results indicate that although increasing the inlet water temperature can prolong the heat release time of the device, it can also weaken the heat release effect relatively. The effective heat release times for the three heat release conditions are 43,910 s, 48,325 s, and 39,800 s, respectively, with effective heat release amounts of 39,508 kJ, 36,004 kJ, and 25,137 kJ, and effective heat release efficiencies of 82.13%, 75.01%, and 52.37%, respectively. Therefore, appropriately increasing the inlet water temperature can help to extend the effective heat release time, but it will simultaneously reduce the effective heat release amount and efficiency of the device. When the inlet water temperature is reduced from 35 ℃ to 30 ℃ or 25 ℃, the effective heat release amounts of the device increase by 43.23% or 57.17%。

Preprints (www.preprints.org) | NOT PEER-REVIEWED | Posted: 18 April 2023 doi:10.20944/preprints202304.0481.v1

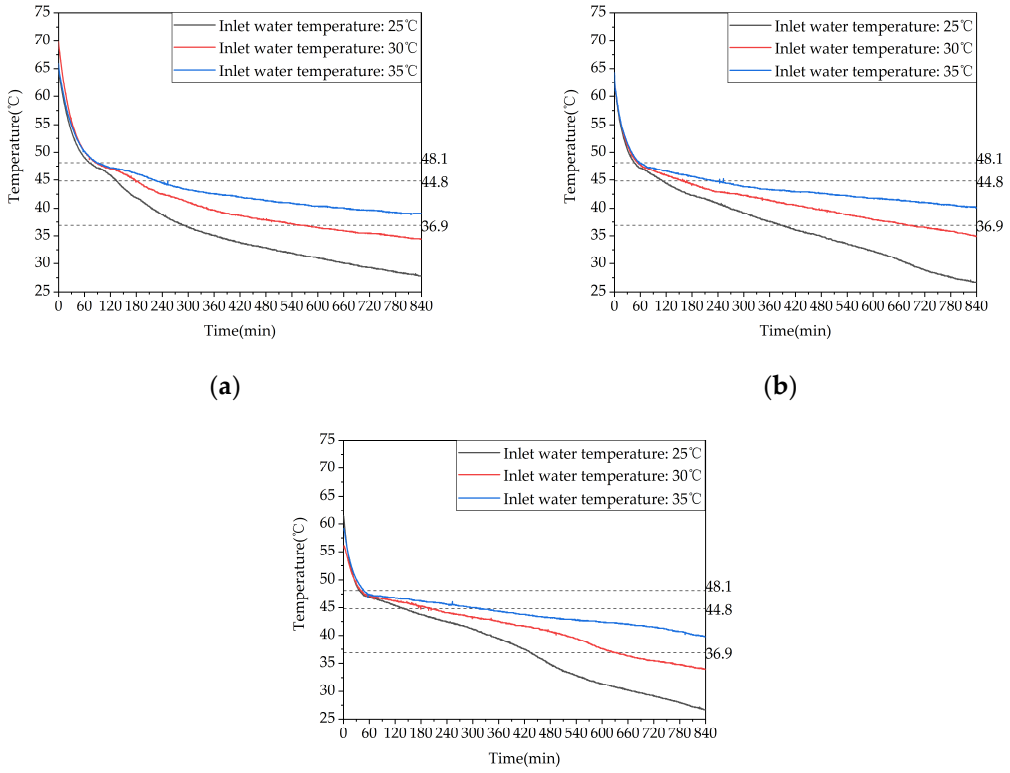

Figure 12. Temperature variation inside the phase change heat storage unit at typical locations under different Heat storage conditions: (a) Measuring point 13; (b) Measuring point 17; (c) Measuring point 21.

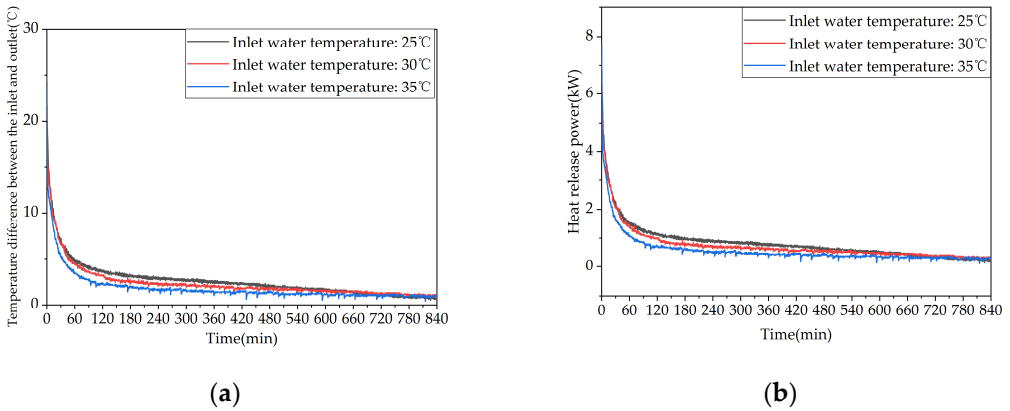

Figure 13. Heat release performance of the device at different inlet water temperatures: (a) Temperature difference between inlet and outlet; (b) Instantaneous heat release power.

4.3.3. Heat release performance of domestic hot water

To investigate the effect of inlet water temperature on the heat release performance of a phase-change storage device for domestic hot water, experiments were conducted on the Heat release conditions of domestic hot water at inlet temperatures of 25℃ and 30℃, with a controlled inlet flow rate of 0.08 m³/h. Figure 14 shows the temperature trend of heat release at different measurement points inside the phase-change storage device over time. The results indicate that when the inlet water temperature was increased from 25℃ to 30℃, the time taken for measurement point 1 to start phase change was prolonged by 18.2%, i.e., from 66 minutes to 77 minutes. Thus, it can be concluded that raising the inlet water temperature can effectively prolong the heat release time.

Preprints (www.preprints.org) | NOT PEER-REVIEWED | Posted: 18 April 2023 doi:10.20944/preprints202304.0481.v1

Figure 15 shows the variations in outlet water temperature and instantaneous heat release power of the device over time at different inlet water temperatures. As shown in Figure 15(a), the trends of outlet water temperature changes are consistent for the two working conditions. The outlet water temperature decreases gradually with the increase of heat exchange time, and the rate of temperature drop decreases gradually. The effective heat release durations of the two working conditions are 69 minutes and 186 minutes, respectively, providing 92 L and 248 L of hot water above 37 ℃. The trends of instantaneous heat release power for both working conditions are consistent, as shown in Figure 15(b), with a rapid initial decrease rate followed by a gradual slowing. The instantaneous heat release power decreases with increasing temperature. The effective heat release amounts are 6905 kJ and 10491 kJ, respectively. Therefore, it is evident that increasing the inlet water temperature can significantly increase the effective heat release duration and the effective heat release amount of the device. When the make-up water temperature is raised from 25 ℃ to 30 ℃, the effective heat release amount of the device increases by 35.23%.

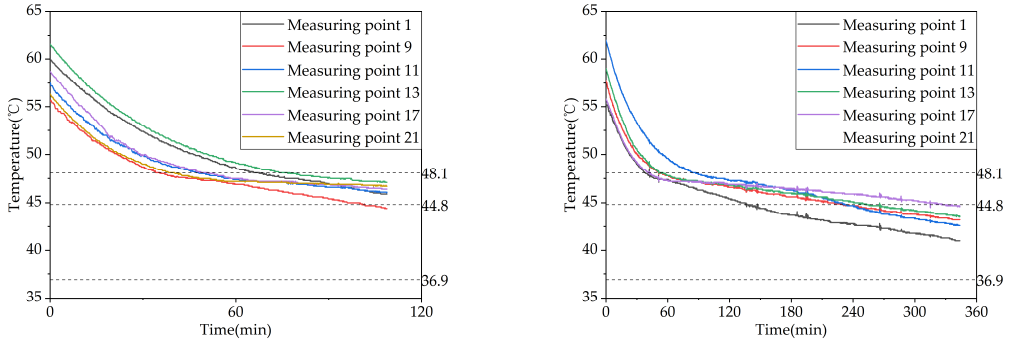

Figure 14. Temperature variation inside the phase-change storage device for domestic hot water under different inlet water temperatures: (a) Inlet water temperature: 25 ℃; (b) Inlet water temperature: 25℃.

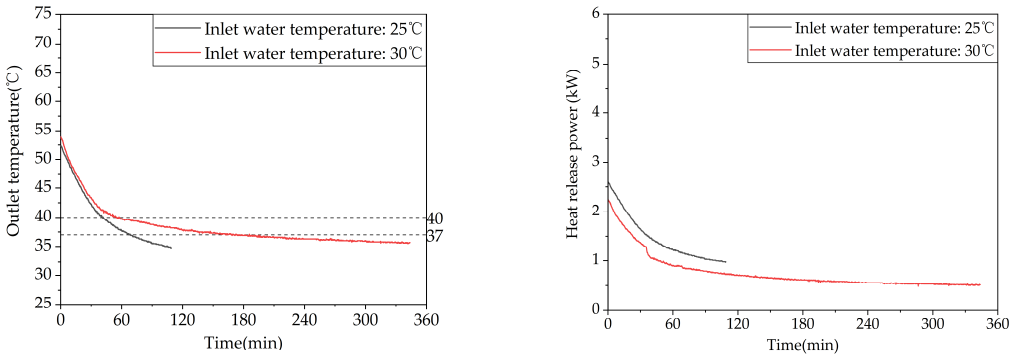

Figure 15. Heat release performance of the device at different inlet water temperatures: (a) Temperature difference between inlet and outlet; (b) Instantaneous heat release power.

4.4. Inlet flow rate

4.4.1. Heat storage performance

To investigate the impact of heat storage flow rate on the heat storage performance of a phase-change heat storage system, experiments were conducted under three different flow rates of 0.18 m^3/h, 0.27 m^3/h, and 0.36 m^3/h, all at an inlet water temperature of 68 ℃. These corresponded to test conditions 4, 3, and 6, as presented in Table 4. Figure 16 shows the temperature rise difference among three typical operating conditions along the same tube position. The results reveal that the start time

Preprints (www.preprints.org) | NOT PEER-REVIEWED | Posted: 18 April 2023 doi:10.20944/preprints202304.0481.v1

of phase change increases with the distance between the measurement point and the thermal fluid inlet, while it decreases with increasing flow rate. When the heat storage inlet flow rate is increased from 0.18 m³/h to 0.27 m³/h, the storage start time at points 13, 17, and 21 decreases by 6.1%, 8.8%, and 15.9%, respectively. Similarly, when the heat storage inlet flow rate is further increased from 0.27 m³/h to 0.36 m³/h, the storage start time at points 13, 17, and 21 decreases by 15.2%, 13.5%, and 17.8%, respectively. Furthermore, when the heat storage inlet flow rate is increased from 0.18 m³/h to 0.36 m³/h, the storage start time at points 13, 17, and 21 decreases by 20.4%, 21.1%, and 30.8%, respectively. These results indicate that increasing the inlet flow rate can enhance the heat storage performance, although its effect on improving the heat storage rate is limited compared to increasing the inlet water temperature.

Figure 17 shows the variation of the temperature difference between the inlet and outlet of the system with time for different inlet water flow rates. As depicted in the figure, the temperature differences at the end of the charging process for the three operating conditions are 2.0°C, 1.2°C, and 0.4°C, respectively. With an increase in the inlet water flow rate, the temperature difference gradually decreases. This is because the increased flow rate leads to a shorter time for the hot water to enter and exit the system, resulting in a shorter time for heat exchange between the phase change material and the fluid. The total stored energy for the three operating conditions is 43933 kJ, 48002 kJ, and 45980 kJ, respectively, with an average heat storage power of 1.53 kW, 1.67 kW, and 1.60 kW. Increasing the water flow rate from 0.18 m³/h to 0.27 m³/h or 0.36 m³/h only increased the stored energy of the system by 9.26% or 4.66%. Therefore, increasing the inlet water flow rate can increase the stored energy of the system, but the effect is limited.

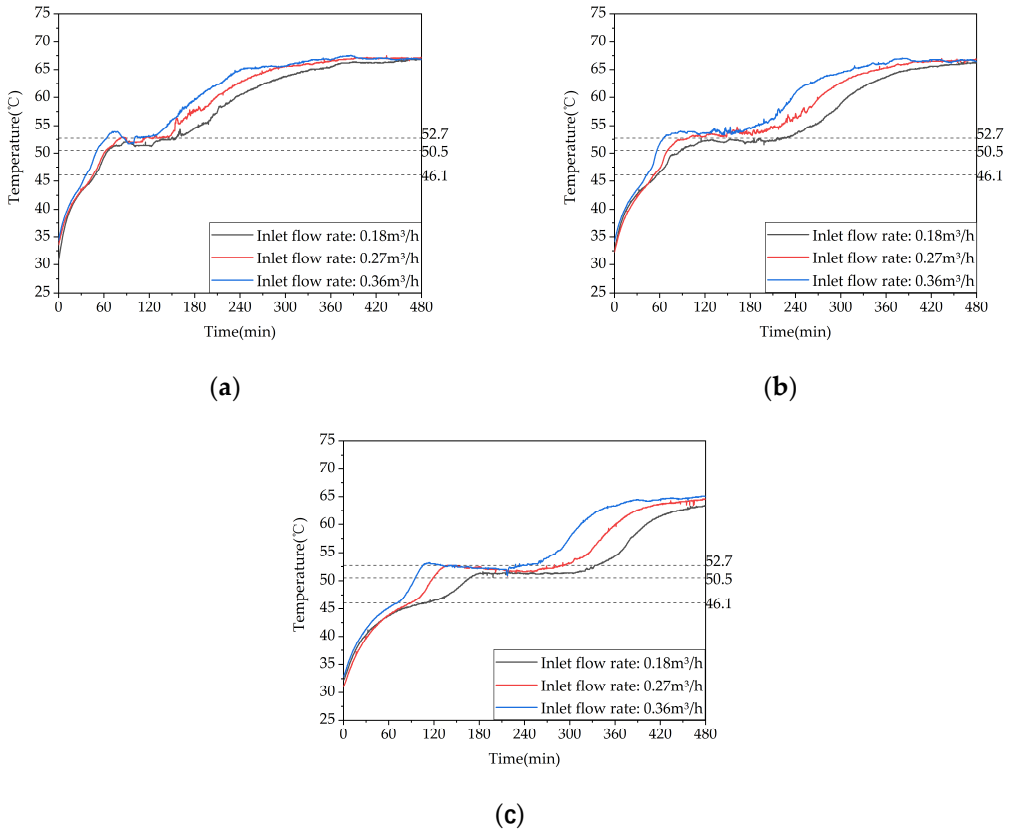

Figure 16. Temperature variation inside the phase change heat storage unit at typical locations under different Heat storage conditions: (a) Measuring point 13; (b) Measuring point 17; (c) Measuring point 21.

Preprints (www.preprints.org) | NOT PEER-REVIEWED | Posted: 18 April 2023 doi:10.20944/preprints202304.0481.v1

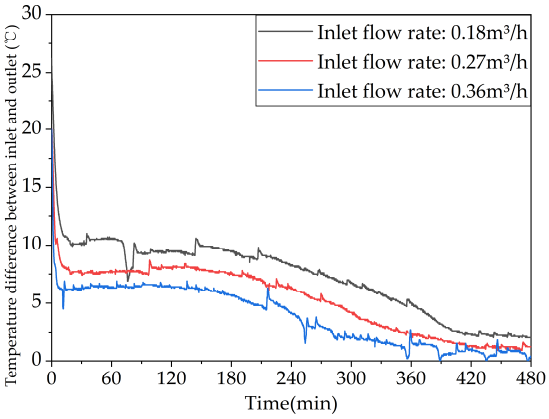

Figure 17. Different trends of the temperature difference between the inlet and outlet of the device over time under different inlet flow rates.

4.4.2. Heat release performance of heating

To investigate the influence of inlet flow rate on the heat release performance of a phase change heat storage system, experiments were conducted on the heating and Heat release conditions of inlet flow rates of 0.18 m³/h, 0.27 m³/h, and 0.36 m³/h, where the inlet water temperature was controlled at 30 ℃. These correspond to the test conditions 10, 8, and 11 listed in Table 5. Figure 18 shows a comparison of temperature differences at typical positions along the same pipe for the three working conditions. From the figure, it can be seen that the starting times of phase change were almost identical for all measuring points under the three working conditions. At the end of the heat release process, the temperatures at the measuring points decreased with increasing flow rate, but the difference was not significant. When the heat release inlet flow rate was increased from 0.18 m³/h to 0.27 m³/h, the time taken for measuring points 13, 17, and 21 to reach the heat release termination temperature was reduced by 3.2%, 7.8%, and 12.1%, respectively. When the heat release inlet flow rate was further increased from 0.27 m³/h to 0.36 m³/h, the time taken for measuring points 13, 17, and 21 to reach the heat release termination temperature was reduced by 2.8%, 2.2%, and 0.3%, respectively. When the heat release inlet flow rate was increased from 0.18 m³/h to 0.36 m³/h, the time taken for measuring points 13, 17, and 21 to reach the heat release termination temperature was reduced by 5.9%, 9.8%, and 12.4%, respectively. These results suggest that increasing the inlet flow rate has a limited effect on improving the heat release efficiency of the system.

Figure 19 shows the variation trends of the device's inlet-outlet temperature difference and instantaneous heat release power over time at different inlet water flow rates. As shown in Figure 19(a), the inlet-outlet water temperature differences of the three working conditions at the end of heat release are 1.4℃, 1.0℃, and 0.9℃, respectively, indicating that the inlet-outlet water temperature difference decreases gradually with the increase of inlet water flow rate. This is because the increased inlet water flow rate leads to a shorter time for hot water to enter and exit the device, and a shorter time for heat exchange between the heat-carrying fluid and the phase change material, resulting in a lower outlet water temperature. The inlet-outlet water temperature differences of working conditions 10 and 8 are very close, indicating that increasing the flow rate has limited improvement on the device's heat release performance. As shown in Figure 19(b), the instantaneous heat release power curves of the three working conditions are very close, and the instantaneous heat release power of working condition 11 with the highest inlet water flow rate is slightly higher than the other two working conditions. When the heat release rate is 0.18m³/h and 0.27m³/h, the effective heat release times are 49230s and 48325s, the effective heat release amounts are 33164kJ and 36004kJ, and the effective heat release efficiencies are 69.09% and 75.01%, respectively. When the heat release rate is 0.36m³/h, the instantaneous heat release power of the device is still greater than the room's heat load at the end of the heat release experiment, so its effective heat release time is greater than 50400s, the effective heat release amount is greater than 37554kJ, and the effective heat release efficiency is greater than 78.23%. When the heat release rate is increased from 0.18m³/h to 0.27m³/h, the effective heat

Preprints (www.preprints.org) | NOT PEER-REVIEWED | Posted: 18 April 2023 doi:10.20944/preprints202304.0481.v1

release amount of the device only increases by 8.56%. It can be concluded from the above data that increasing the inlet water flow rate helps to improve the effective heat release amount and efficiency of the device, and at the same time, prolong the effective heat release time, but the improvement effect is relatively limited.

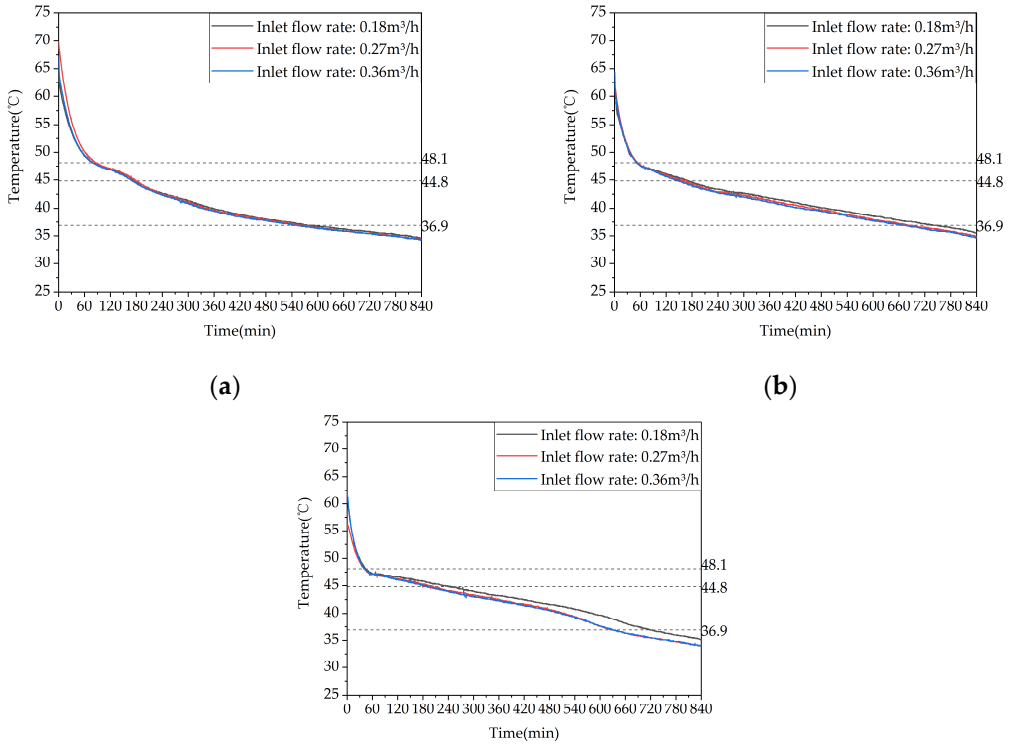

Figure 18. Temperature variation inside the phase change heat storage unit at typical locations under different Heat storage conditions: (a) Measuring point 13; (b) Measuring point 17; (c) Measuring point 21.

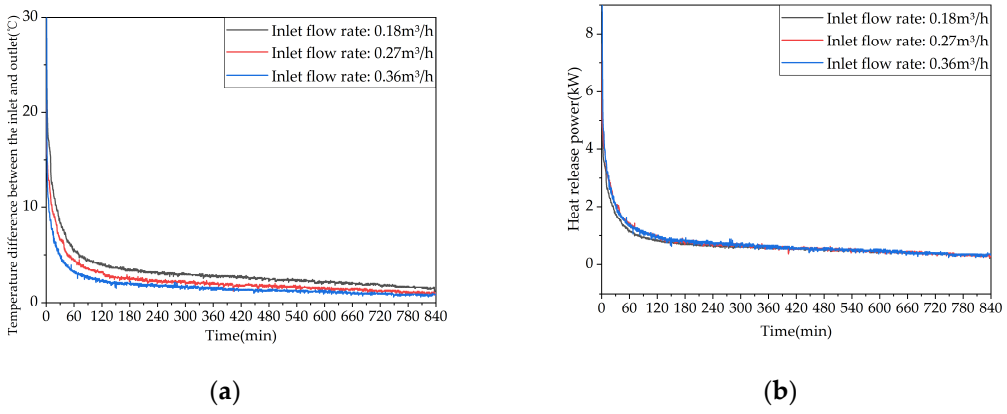

Figure 19. Heat release capacity of the device at different inlet flow rates.: (a) Temperature difference between inlet and outlet; (b) Instantaneous heat release power.

4.4.3. Heat release performance of domestic hot water

To investigate the effect of the inlet flow rate on the heat release performance of the phase change device, the hot water heat release tests were carried out for the three inlet flow rates of 0.05 m³/h, 0.08 m³/h, and 0.11 m³/h, corresponding to operating conditions 14-16 in Table 5, with a controlled inlet temperature of 25 ℃.

Preprints (www.preprints.org) | NOT PEER-REVIEWED | Posted: 18 April 2023 doi:10.20944/preprints202304.0481.v1

Figure 20 shows the variation of temperature at different measurement points inside the phase change TES unit with time, under different inlet water flow rates. When the inlet water flow rate is 0.05 m³/h, measurement point 1 starts to undergo phase change 78 minutes after the onset of heat release. When the inlet water flow rate is 0.08 m³/h, measurement point 1 starts to undergo phase change 66 minutes after the onset of heat release. When the inlet water flow rate is 0.11 m³/h, measurement point 1 starts to undergo phase change 66 minutes after the onset of heat release. Increasing the inlet water flow rate from 0.05 m³/h to 0.08 m³/h shortens the duration of phase change at the measurement point 1 by 15.4%, indicating that increasing the inlet water flow rate can accelerate the heat release process, but its effectiveness is limited.

Figure 21 shows the variations of the outlet water temperature and instantaneous heat release power with time at different inlet water flow rates. As shown in Figure 21(a), the outlet water temperature decreases gradually with increasing heat exchange time for all three operating conditions, and the rate of temperature drop decreases gradually as well. The effective heat release durations for the three conditions are 156 minutes, 69 minutes, and 45 minutes, which can provide 130 L, 92 L, and 82.5 L of hot water above 37 ℃, respectively. Figure 21(b) shows that the heat release amounts for the three conditions are 9855 kJ, 6935 kJ, and 5955 kJ, respectively, and the trends of the heat release power curves are consistent, with a rapid initial decline rate and a gradual flattening in the later stage. When the inlet water flow rate decreases from 0.11 m³/h to 0.08 m³/h or 0.05 m³/h, the effective heat release amount of the device increases by 16.46% or 65.49%, respectively. Therefore, the flow rate has a significant impact on the instantaneous heat release power, which increases with the increase of the flow rate. It can also be seen that the lower the inlet water flow rate, the higher the initial outlet water temperature corresponding to the heat release, because the decrease in inlet water flow rate will increase the time for hot water to enter and exit the device, and the time for heat exchange between the hot fluid and the phase change material, thereby increasing the outlet water temperature.

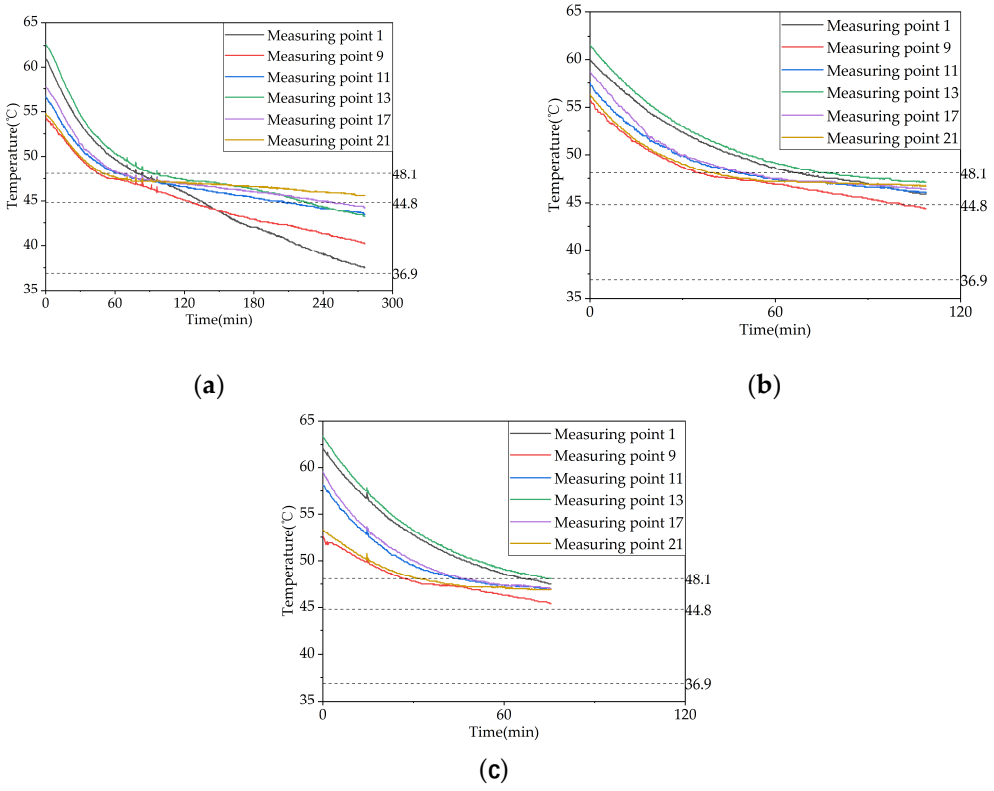

Figure 20. Temperature variation inside the phase-change storage device for domestic hot water under different inlet water temperatures: (a) Inlet flow rate: 0.05 m³/h; (b) Inlet flow rate: 0.08 m³/h; (c) Inlet flow rate: 0.11 m³/h

Preprints (www.preprints.org) | NOT PEER-REVIEWED | Posted: 18 April 2023 doi:10.20944/preprints202304.0481.v1

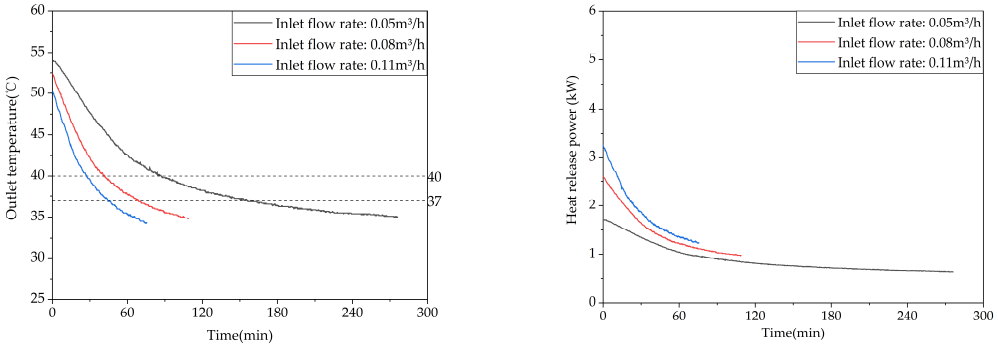

(**a**) (**b**)

Figure 21. Heat release capacity of the device at different inlet flow rates.: (a) Temperature difference between inlet and outlet; (b) Instantaneous heat release power.

4.5 Type of heat storage

To investigate the influence of the type of heat storage on the heat storage performance of phase change heat storage units, an experimental study was conducted on two Heat storage conditions, i.e., conditions 5 and 6 in Table 4, with the electric heating plate set at 68°C and the inlet water temperature controlled at 68°C with a flow rate of 0.36 m³/h, one with the electric heating plate on and one with it off. The temperature difference between the two conditions was compared and analyzed at a typical position along the same pipeline.

As shown in Figure 22, the time required for measuring point 13 to complete the phase change above the termination temperature was 61 min and 108 min for the two conditions, respectively. For measuring point 17, it was 85 min and 130 min, and for measuring point 21, it was 106 min and 243 min. When the electric heating plate was turned on, the times for measuring points 13, 17, and 21 to complete the phase change were reduced by 43.5%, 34.6%, and 56.4%, respectively. Therefore, it is clear that turning on the electric heating plate significantly shortens the time required for the phase change heat storage process.

Figure 23 shows the variation trend of the inlet-outlet temperature difference of the unit over time under different heat storage methods. It can be seen from the figure that it took 228 minutes for the temperature difference to drop below 0.5°C in condition 5 and 474 minutes in condition 6, with average heat storage powers of 1.74 kW and 1.60 kW, respectively. The temperature difference decreased significantly faster with the electric heating plate turned on than with only hot water storage, as turning on the electric heating plate significantly accelerated the melting process of the phase change heat storage unit, reducing the time for the unit to be in the latent heat storage state. The unit prioritizes completing the phase change process before returning to the sensible heat storage state, where the heat storage effect is mainly influenced by the temperature difference between the inlet water and the unit. As the unit temperature rises, the inlet-outlet temperature difference gradually decreases.

Preprints (www.preprints.org) | NOT PEER-REVIEWED | Posted: 18 April 2023 doi:10.20944/preprints202304.0481.v1

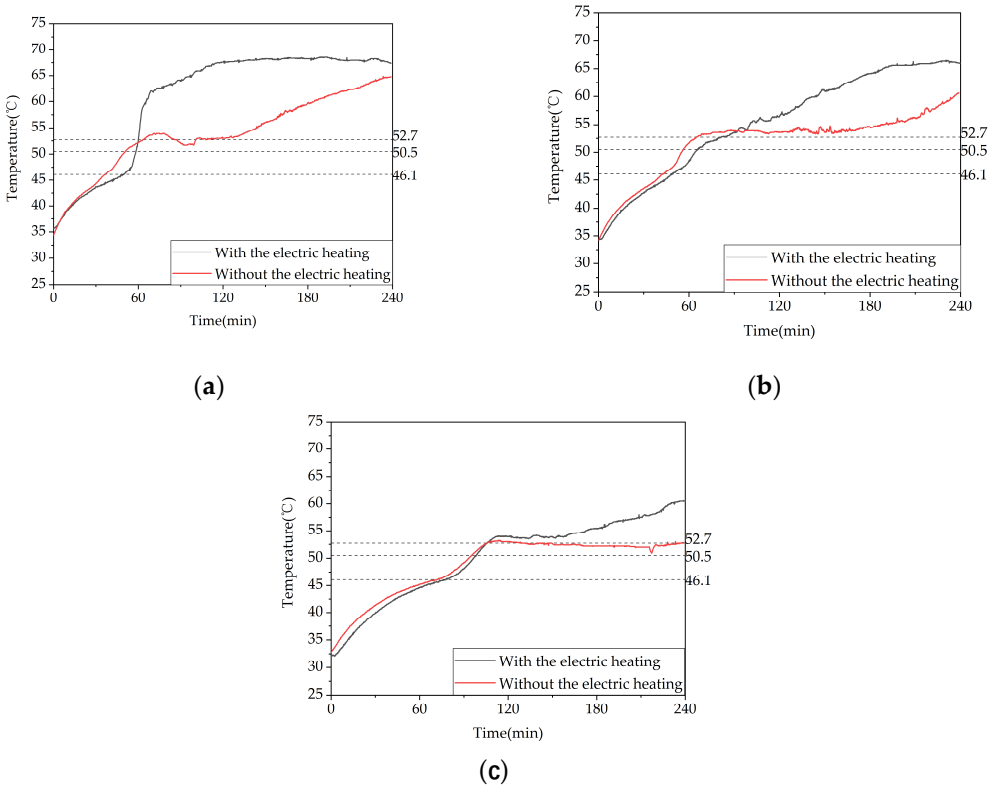

Figure 22. Temperature variation inside the phase change heat storage unit at typical locations under different Heat storage conditions: (a) Measuring point 13; (b) Measuring point 17; (c) Measuring point 21.

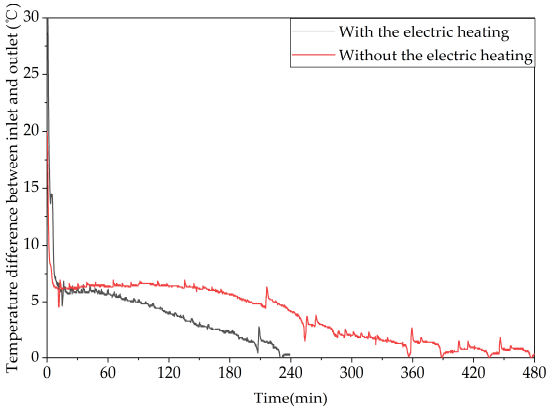

Figure 23. Different trends of the temperature difference between the inlet and outlet of the device over time under different heating methods.

4.6 Initial temperature of the device

To investigate the effect of initial temperature on the heat release performance of the phase change device, the inlet water temperature was controlled at 30℃ and the inlet water flow rate was 0.27 m³/h. Experimental studies were conducted on three heating conditions with initial temperatures of 53℃, 58℃, and 63℃, corresponding to conditions 12, 13, and 8 in Table 5.

Figure 24 presents a comparative analysis of the temperature rise differences at a typical position on the same row of tubes for the three conditions. The figure shows that the higher the initial heat release temperature, the longer the time it takes for the various measuring points inside the device to reach the end of the phase change. When the initial heat release temperature was increased from 53 ℃ to 58℃, the time it took for measuring points 13, 17, and 21 to reach the heat release termination

 doi:10.20944/preprints202304.0481.v1

temperature was extended by 26.1%, 16.9%, and 24.7%, respectively. When the initial heat release temperature was increased from 58℃ to 63℃, the time it took for points 13, 17, and 21 to reach the heat release termination temperature was extended by 8.9%, 7.1%, and 15.7%, respectively. When the initial heat release temperature was increased from 53℃ to 63℃, the time it took for points 13, 17, and 21 to reach the heat release termination temperature was extended by 37.2%, 25.2%, and 44.3%, respectively. Therefore, increasing the initial heat release temperature of the device means increasing its energy storage capacity, which can extend the heat release time. However, once the temperature is raised to a certain level, the improvement effect will gradually diminish.

Figure 25 shows the variation trends of the inlet-outlet temperature difference and the instantaneous heat release rate of the device with different initial temperatures. As shown in Figure 25(a), increasing the initial heat release temperature leads to an increase in the inlet-outlet water temperature difference of the device, which is more significant in the early stage of heat release. This is because a higher initial temperature means that the device stores more heat. During heat release, the larger temperature difference between the device and cold water results in better heat transfer and lower outlet temperature. As the heat release process proceeds, the phase change material in the device gradually solidifies, and the natural convection effect weakens, causing the inlet-outlet water temperature difference to stabilize gradually. In the later stage of heat release, the differences in the inlet-outlet water temperature difference among the three working conditions are negligible, and the inlet-outlet water temperature differences of the three working conditions at the end of heat release are 0.8 ℃, 0.9 ℃, and 1.0 ℃ for conditions 7, 8, and 9, respectively. As shown in Figure 25(b), the instantaneous heat release rates of the three working conditions are higher for those with higher initial temperatures during the early stage of heat release, following the same trend as the inlet-outlet temperature difference. As the heat release process proceeds, the heat release rates decrease gradually for all three conditions. The effective heat release times of the three heat release conditions are 42180 s, 44250 s, and 48325 s, respectively, and the effective heat release amounts of the device are 28080 kJ, 31439 kJ, and 36004 kJ, respectively, with effective heat release efficiencies of 85.76%, 74.16%, and 75.01%, respectively. When the initial temperature of the device is increased from 53 ℃ to 58 ℃ or 63 ℃, the effective heat release amount of the device is increased by 11.96% or 28.22%, respectively. This indicates that increasing the initial temperature can enhance the early-stage heat release performance of the device, but overall, the improvement in the heat release performance of the device is not significant.

Preprints (www.preprints.org) | NOT PEER-REVIEWED | Posted: 18 April 2023 doi:10.20944/preprints202304.0481.v1

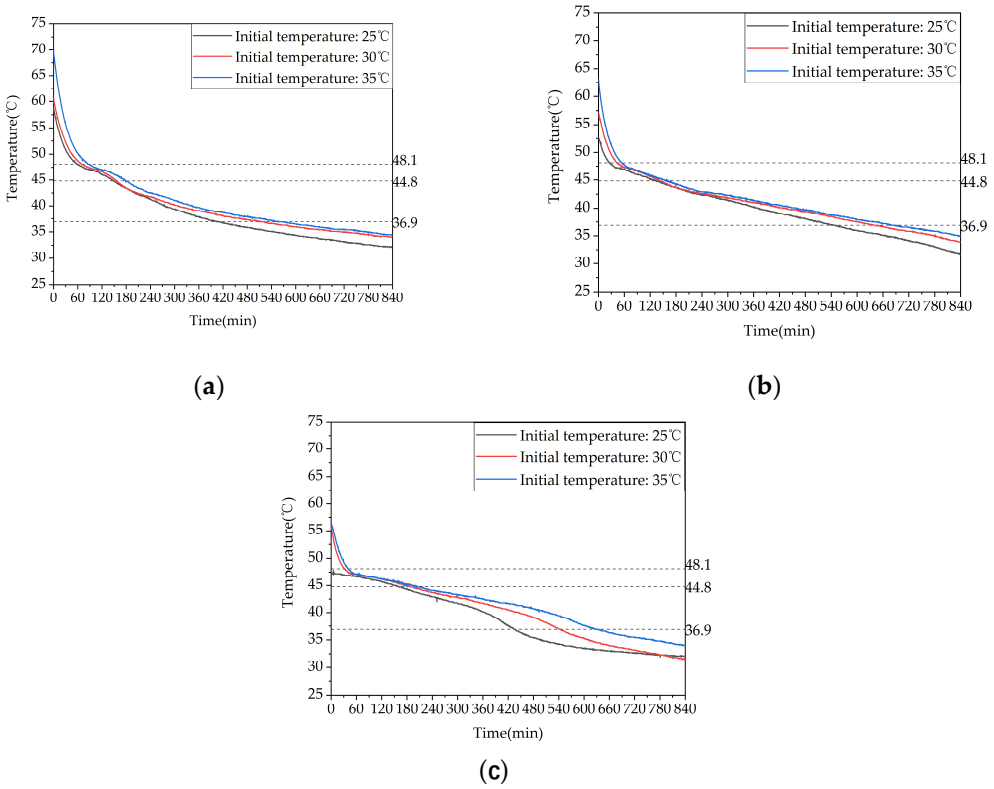

Figure 24. Temperature variation inside the phase change heat storage unit at typical locations under different Heat storage conditions: (a) Measuring point 13; (b) Measuring point 17; (c) Measuring point 21.

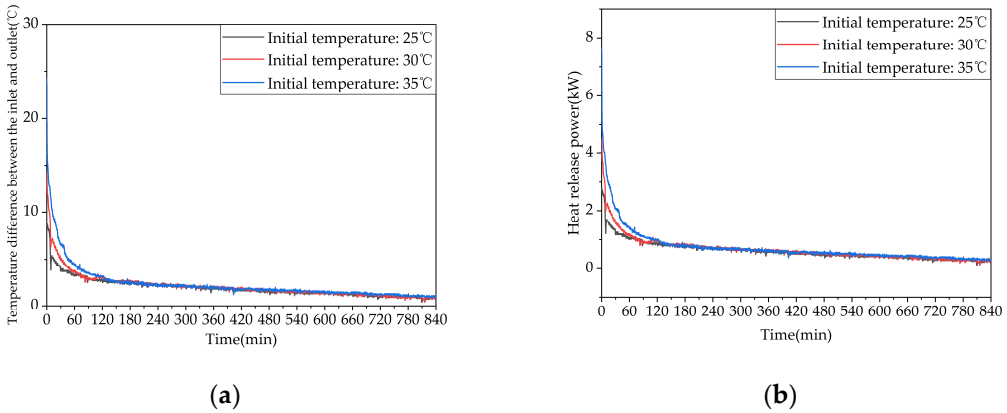

Figure 25. Heat release capacity of the device at Initial temperature of the device: (a) Temperature difference between inlet and outlet; (b) Instantaneous heat release power.

5. Optimizing Phase Change TES System Performance in Energies Journal Style

In this section, the impact of various factors on the TES process in the system was investigated using numerical simulation, providing a theoretical basis for the structural design and practical application of phase change TES systems.

5.1 Fin arrangements

To investigate the influence of fin arrangement on the phase change heat storage process, device models with aligned and staggered fin arrangements were simulated to analyze the characteristics of liquid-phase fraction and temperature distribution at different times, and to compare the differences in the required time for completing the phase change heat storage.

Preprints (www.preprints.org) | NOT PEER-REVIEWED | Posted: 18 April 2023 doi:10.20944/preprints202304.0481.v1

Figure 26 shows the simulation results of the two different fin arrangements. As shown in Figure 26(a), the distribution of the melting region in the device with aligned fins is different from that in the device with staggered fins. The unfused area between the coils in the device with aligned fins is circular, while in the device with staggered fins, it is semicircular. However, the liquid-phase fraction of the two devices is almost the same at the same time, and both devices have a liquid-phase fraction of 0.95 at the end of the heat storage process. As shown in Figure 26(b), there are several small areas with relatively low temperatures between the coils in the device with aligned fins, while the temperature distribution inside the device with staggered fins is more uniform at the same time. After 4 hours of heat storage, the device with aligned fins has the highest average temperature, and the enclosed area formed by the fins and coil bends has better heat transfer efficiency and therefore heats up faster. When the heat storage time reaches 6 hours, the high-temperature area between the coils in the device with aligned fins is rectangular, while the high-temperature area between the coils in the device with staggered fins is trapezoidal with a wider upper part and a narrower lower part. The average temperature of both finned devices is around 59.7°C. When the heat storage time reaches 8 hours, the average temperatures of the two devices are 61.55°C and 61.59°C, respectively, and the device with staggered fins exhibits the best melting effect. Based on the entire phase change heat storage process, it can be concluded that the melting of the PCM in the heat storage device is mainly influenced by the distance to the pipe wall and fins, and there is no significant difference in melting efficiency between devices with aligned or staggered fins. The device with staggered fins has a slightly better heat storage effect than the device with aligned fins, but the difference is not significant.

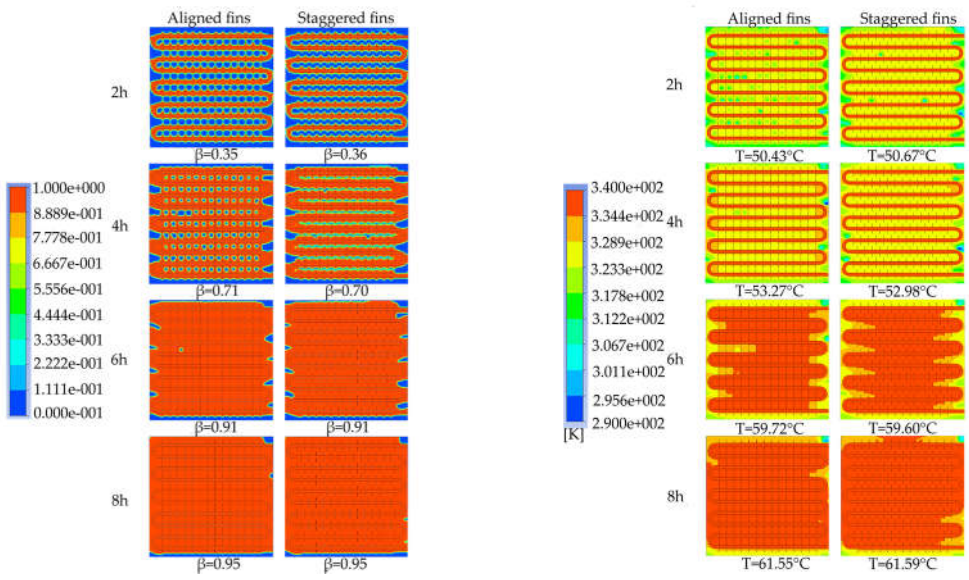

(**a**) (**b**)

Figure 26. The simulated contour maps for different fin arrangement configurations: (a) Liquid phase fraction; (b) Device temperature.

Figure 27 shows the variation of the liquid fraction and average temperature of a phase change TES unit with different fin arrangements over time. The gray line represents the liquid fraction curve for the straight fins, while the red line corresponds to the temperature curve of the TES unit. The time required for 50% and 90% of the PCM to melt inside the TES unit with the two fin arrangements is 10170 s and 20920 s, and 10050 s and 21190 s, respectively. During the entire charging process, the liquid fraction curves of the TES unit with the two fin arrangements almost overlap, indicating that the difference in melting performance of the aligned or staggered fin arrangement is negligible. From the graph, it can be seen that the time required for the average temperature of the TES unit to reach 50℃ with the two fin arrangements is 6020 s and 5280 s, respectively. During the entire charging process, the average temperature curves of the TES unit with the two fin arrangements are almost the

Preprints (www.preprints.org) | NOT PEER-REVIEWED | Posted: 18 April 2023 doi:10.20944/preprints202304.0481.v1

same, and the average temperature of the TES unit with the staggered fins is slightly higher than that with the aligned fins most of the time.

Therefore, it can be concluded that the TES unit with the staggered fin arrangement has better heat storage performance than the TES unit with the aligned fin arrangement, but the difference is not significant. Considering that the length of the fins is limited to less than half the tube spacing for aligned fin arrangements, while the length of the fins and tube spacing can be adjusted over a wider range for staggered fin arrangements, the fins in the TES unit should be preferably arranged in a staggered manner. However, if the conditions are restricted, the aligned fin arrangement can also be used, and the heat storage performance of the TES unit with the two fin arrangements will not differ significantly.

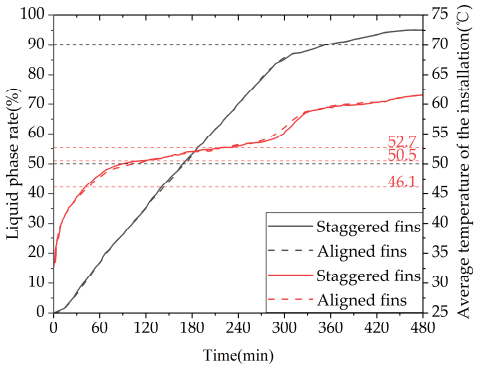

Figure 27. The liquid fraction and average temperature of the phase change heat storage unit vary with different fin arrangements.

5.2 Fin arrangements

To investigate the effect of fin spacing on the heat storage process, simulation models with fin spacings of 30mm, 50mm, and 70mm were selected to analyze the liquid fraction and temperature distribution characteristics at different times and compare the differences in the required time for completing the phase change heat storage.

Figure 28 shows the simulated cloud maps of the devices with different fin spacings. As shown in Figure 28(a), the smaller the fin spacing, the fewer unmelted areas in the device, and the faster the melting rate of the PCM. When the heat storage duration reached 6 hours, the liquid fractions of the three working conditions were similar, and around 90% of the PCMs in the devices had melted. However, the device with denser fins had a higher liquid fraction. When the heat storage duration reached 8 hours, the liquid fractions of the devices with fin spacings of 50mm and 70mm were both 0.95, while the device with a fin spacing of 30mm had a slightly higher liquid fraction of 0.96. The figure also shows that the smaller the fin spacing, the smaller the unmelted area at the bottom, side walls, and corners of the device when the melting process was completed. As shown in Figure 28(b), the PCM near the fins and coils heated up first, while the temperature near the bent tubes and the corners of the device far from the heat exchange tubes and without fins was relatively low. When the heat storage duration reached 6 hours, the average temperature of the devices with fin spacings of 30mm and 50mm was around 60℃, while the device with a fin spacing of 70mm had a lower average temperature of 57.9℃. When the heat storage duration reached 8 hours, the temperature distribution inside the device with a smaller fin spacing was more uniform, and the average temperature of the device was higher, resulting in a larger heat storage capacity. The figure also shows that during the initial stage of heat storage, the temperature distribution inside the device was high in the middle and low around the periphery, while in the later stage of heat storage, the temperature at the top of the device was significantly higher than at the bottom. This was because during the initial stage of heat storage, the PCM in the device was in a solid state, and the heat was transferred through conduction. As the PCM gradually melted, the liquid PCM gathered at the top of the device due to the density difference, while the solid PCM sank due to gravity, resulting in a temperature stratification phenomenon in the vertical direction during the later stage of heat storage.

Preprints (www.preprints.org) | NOT PEER-REVIEWED | Posted: 18 April 2023 doi:10.20944/preprints202304.0481.v1

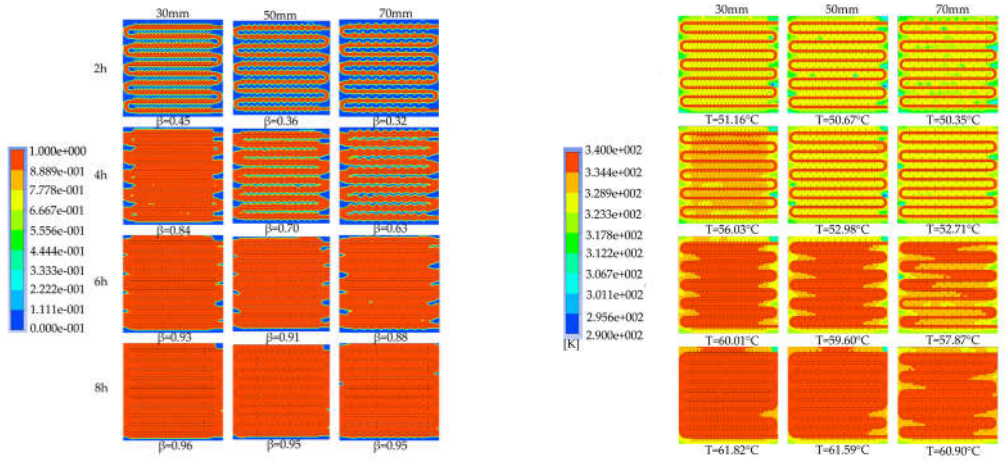

(**a**) (**b**)

Figure 28. The simulated contour maps for different fin spacing arrangements: (a) Liquid phase fraction; (b) Device temperature.

Figure 29 shows the variation curves of liquid fraction and average temperature with time for the phase change TES device under different fin spacings. The gray line represents the liquid fraction curve, and the red line represents the device temperature curve. It can be observed that there are differences in the rate of change of liquid fraction under different fin spacings, but the overall trend is consistent: the melting rate of the device is fast in the early stage of TES, and a clear inflection point appears in the later stage, with the liquid fraction curve relatively flat and the melting rate decreasing. This is because the solid-PCM dominates the device in the early stage, and the presence of fins increases the heat exchange area, resulting in a faster melting rate. In the later stage, most of the PCM around the fins and pipelines has melted, and the heat transfer coefficient of the PCM is small, resulting in a significant slowdown in the melting rate. The time required for 50% of the PCM in the device to melt under three different fin spacings is 7980s, 9940s, and 11170s, respectively. When the fin spacing is reduced from 70mm to 50mm or 30mm, the time required for 90% of the PCM to melt in the device is reduced by 11.01% and 28.56%, respectively. The time required for 90% of the PCM to melt in the device is 19140s, 21190s, and 22900s, respectively. When the fin spacing is reduced from 70mm to 50mm or 30mm, the time required for 90% of the PCM to melt in the device is reduced by 7.47% and 16.42%, respectively. It can be seen from the figure that there are differences in the average rate of change of the device under different fin spacings, but the overall trend is consistent. There are two clear inflection points during the TES stage: the first one appears when the solid-liquid phase change is completed, at which point the device changes from latent heat storage to sensible heat storage, and the temperature rise rate increases. The second one appears when the average temperature of the device is around 60℃ in the later stage of TES. This is because most of the PCM inside the device has melted, and the temperature distribution is more uniform than in the early stage, resulting in weaker natural convection. Heat transfer mainly occurs in the form of conduction, and the heat transfer coefficient of the PCM is small, resulting in a significant slowdown in the melting rate. The time required for the average temperature of the device under three different fin spacings to reach 60℃ is 21510s, 23710s, and 25110s, respectively. When the fin spacing is reduced from 70mm to 50mm or 30mm, the time required for the average temperature of the device to reach 60℃ is reduced by 5.58% and 14.34%, respectively.

Given the aforementioned, it can be inferred that for a given Heat storage condition, a smaller fin spacing leads to a faster melting rate of the PCM (PCM), resulting in a shorter completion time of the storage process, a more uniform melting degree of PCM within the device, a higher average temperature of the device, and a greater TES capacity. However, a reduction in the fin spacing will increase the number of fins, thereby reducing the PCM capacity within the device and increasing the manufacturing cost of the fins. Therefore, in practical applications, the choice of fin spacing should be based on a comprehensive consideration of the demand for use and the economic feasibility of the

Preprints (www.preprints.org) | NOT PEER-REVIEWED | Posted: 18 April 2023 doi:10.20944/preprints202304.0481.v1

device. For solar energy-rich regions with support for longer storage times, there is no need for an excessively small fin spacing, whereas, for shorter storage times, a reduction in the fin spacing can be appropriate to enhance the TES performance of the device.

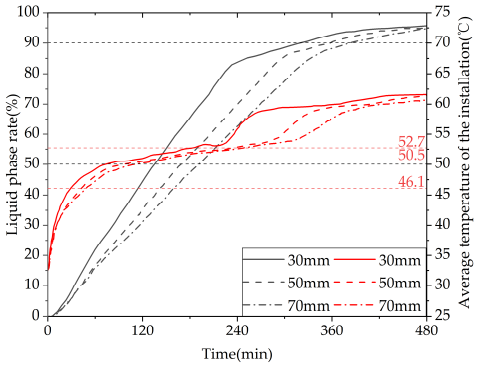

Figure 29. The liquid fraction and average temperature of the phase change heat storage unit vary with different fin spacing.

5.3 Fin thickness

To investigate the effect of fin thickness on the heat storage process, device models with fin thicknesses of 1mm, 2mm, and 3mm were simulated to analyze the characteristics of liquid phase fraction and temperature distribution at different periods. The differences in the required time to complete the phase change heat storage were compared.

Figure 30 shows the simulation cloud maps of the devices under different fin thicknesses. As shown in Figure 30(a), under the same heat storage duration, the thicker the fin thickness, the faster the PCM melts. At 4h of heat storage duration, there are still many unmelted areas between coils in the device with 1mm thick fins, while almost all coils are melted in the device with 3mm thick fins and the liquid phase fraction reaches 0.86. When the heat storage duration is extended to 6h, the melting situation of the devices with 2mm and 3mm thick fins is similar, but both are significantly better than that of the device with 1mm thick fins, and the device with 3mm thick fins still has the highest liquid phase fraction. At 8h of heat storage duration, the liquid phase fraction of the devices with 2mm and 3mm fin thicknesses is both 0.97, slightly higher than that of the device with 1mm fin thickness. In addition, by comparing the liquid phase fraction distribution cloud maps of the three devices at the end of heat storage, it can be observed that the thicker the fin thickness, the smaller the unmelted area at the bottom, side walls, and corners of the device, and the improvement degree is better at the corners than at the bottom. This indicates that increasing the fin thickness can enhance the heat transfer effect of the fins in the fin thickness direction. Overall, it is found that increasing the fin thickness can improve the melting rate of the device, and the improvement effect is more significant in the early stages of heat storage. As shown in Figure 30(b), by comparing the temperature cloud maps after 2h of heat storage, it is found that the temperature distribution inside the device with 1mm thick fins is the most uneven, with multiple small areas of relatively low temperature between coils. After 4h of heat storage, the melting effect of the device with 3mm thick fins is significantly better than that of the other two devices, and the average temperature of the device reaches 58.73℃. The device with 1mm thick fins still has blue low-temperature areas, indicating the worst melting effect and the average temperature of the device is 52.98℃. When the heat storage duration is extended to 6h, the average temperatures of the three devices are all around 60℃, and the temperature of the device with 3mm thick fins reaches as high as 61℃. When the heat storage duration is extended to 8h, the device with the thickest fins has the best melting effect, and for each increase in fin thickness of 1mm, the average temperature of the device increases by 0.46℃ and 0.09 ℃, respectively. Overall, it is found that increasing the fin thickness can improve the average temperature and melting effect of the device, and the improvement effect is more significant in the early and middle stages of heat storage.

Preprints (www.preprints.org) | NOT PEER-REVIEWED | Posted: 18 April 2023 doi:10.20944/preprints202304.0481.v1

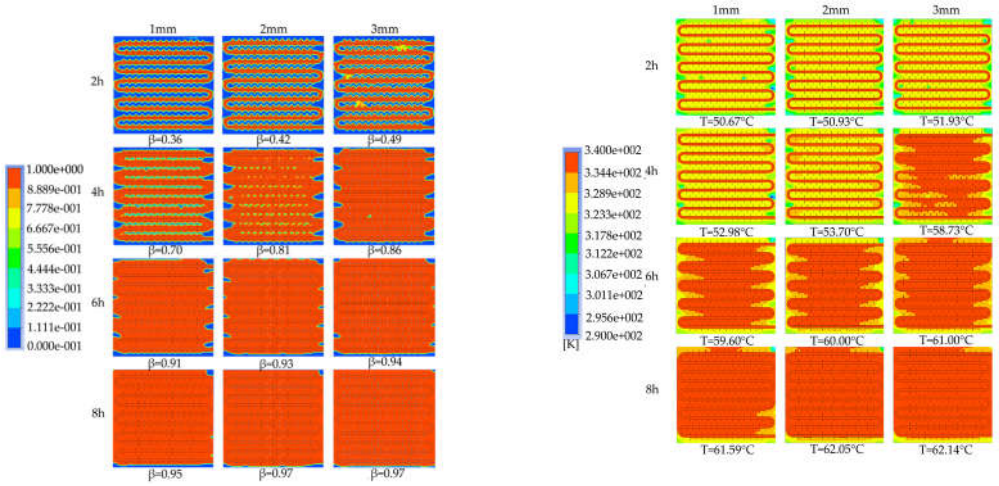

(**a**) (**b**)

Figure 30. The simulated contour maps for different fin thicknesses: (a) Liquid phase fraction; (b) Device temperature.

Figure 31 shows the comparison of the liquid phase and average temperature variation trend for a phase change TES device with different fin thicknesses. The gray line represents the liquid phase comparison curve, while the red line represents the device temperature curve. The melting times of 50% PCMs (PCM) inside the device correspond to three different fin thicknesses of 1 mm, 2 mm, and 3 mm, which are 9940 s, 8580 s, and 7290 s, respectively. When the fin thickness increases from 1 mm to 2 mm or 3 mm, the melting times of 50% PCM inside the device are reduced by 13.68% and 26.66%, respectively. The melting times of 90% PCM inside the device correspond to the three fin thicknesses of 1 mm, 2 mm, and 3 mm, which are 20710 s, 18620 s, and 16760 s, respectively. When the fin thickness increases from 1 mm to 2 mm or 3 mm, the melting times of 90% PCM inside the device are reduced by 10.09% and 19.07%, respectively. In conclusion, increasing the fin thickness can significantly enhance the melting efficiency of the device.

It can be inferred from the above that, under the same Heat storage conditions, an increase in fin thickness leads to a faster melting rate of PCM (PCM), a shorter time required for completing the heat storage process, a more uniform degree of PCM melting at the end of the process, a higher average temperature of the heat storage device, and a greater heat storage capacity. However, increasing the fin thickness reduces the PCM capacity of the device and raises the manufacturing cost of the finned tubes. Therefore, in practical applications, the selection of fin thickness should be based on a comprehensive consideration of the requirements for use and the economic feasibility of the device. For solar-rich regions with relatively long heat storage times, a fin thickness of no more than 2 mm is recommended, whereas, for shorter heat storage times, an increase in fin thickness can be considered to enhance the heat storage performance of the device.

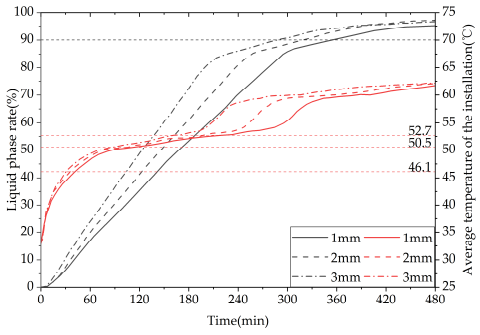

Figure 31. The liquid fraction and average temperature of the phase change heat storage unit vary with different fin thicknesses.

Preprints (www.preprints.org) | NOT PEER-REVIEWED | Posted: 18 April 2023 doi:10.20944/preprints202304.0481.v1

5.4 Inlet flow direction and installation method

To investigate the effects of the flow direction and installation orientation on the phase change heat storage process, we simulated three different device models with different installation methods: vertical installation with the longer side parallel to the gravity direction, horizontal installation with fluid entering from the bottom and exiting from the top, and horizontal installation with fluid entering from the top and exiting from the bottom. We analyzed the characteristics of liquid phase rate and temperature distribution at different time points and compared the differences in the required time for completing the phase change heat storage.

Figure 32 presents the simulation contour maps of the device under different water inlet directions and installation methods. As shown in Figure 32(a), when the heat storage time reached 4 hours, the liquid fraction of the device under the three working conditions was 0.70, 0.73, and 0.81, respectively. When the heat storage time reached 6 hours, the melting situation of the horizontally installed devices was similar, but both were behind the vertically installed device. When the heat storage time reached 8 hours, the liquid fraction of the horizontally installed devices was 0.95, while the vertically installed device reached a high liquid fraction of 0.99, and the remaining unmelted area was mainly distributed in the lower two corners of the device. Overall, the melting effect of the vertically installed device was significantly better than that of the horizontally installed device. Moreover, the heat transfer mode with down-in and up-out in the horizontally installed device was better than the up-in and down-out mode, and the improvement effect was more significant in the early stage of heat storage. As shown in Figure 32(b), when the heat storage time was 2 hours, the temperature distribution of the horizontally installed device with up-in and down-out was the most uneven, with multiple relatively low-temperature small areas between the coils. After 4 hours of heat storage, the average temperature of the device under the three working conditions was around 53 ℃. The average temperature of the horizontally installed device with down-in and up-out was the highest, reaching 53.10 ℃, while that of the vertically installed device was the lowest, at 52.92 ℃. When the heat storage time reached 6 hours, the average temperature of the device under the three working conditions was around 60 ℃. The temperature of the vertically installed device reached the highest at 60.68 ℃, and it had the most uniform temperature distribution among the three devices, followed by the horizontally installed device with down-in and up-out. When the heat storage time reached 8 hours, the melting effect of the vertically installed device was the best, and the average temperatures of the devices under the three working conditions were 61.59 ℃, 61.50 ℃, and 61.68 ℃, respectively.

Based on the overall heat storage process, it can be concluded that the melting effect of the vertically installed device is significantly better than that of the horizontally installed device. This is because the vertically installed device provides a larger spatial scale in the direction of gravity, which is conducive to the formation of natural convection inside the device. For devices installed horizontally, the downflow-upflow heat transfer method performs better than the upflow-downflow method in the early stage of heat storage. However, after a heat storage time exceeding 6 hours, the heat storage effect of the two inflow methods is not significantly different. This is because the hot fluid flows through the longer path of the coil, exchanging heat with the device as it flows, and the fluid temperature inside the pipe gradually decreases. Additionally, due to the density difference between the solid and liquid PCMs, the device experiences temperature stratification, where the upper part of the device has a higher temperature than the lower part during heat storage under the influence of gravity. When the device is horizontally installed, the downflow-upflow heat transfer method can increase the heat transfer temperature difference, thereby improving the heat transfer effect.

Preprints (www.preprints.org) | NOT PEER-REVIEWED | Posted: 18 April 2023 doi:10.20944/preprints202304.0481.v1

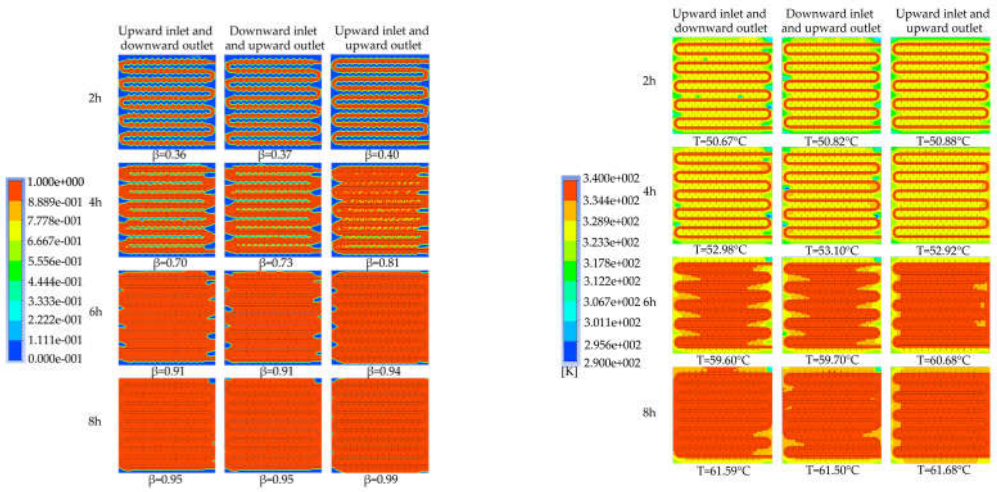

(**a**) (**b**)

Figure 32. Simulated flow visualization under different inlet directions and installation orientations: (a) Liquid phase fraction; (b) Device temperature.

Figure 33 shows the variation curves of liquid fraction and the average temperature of the phase change TES device with different water inlet directions and installation methods over time. The gray line represents the liquid fraction curve, while the red line represents the device temperature curve. The time required for the liquid fraction to reach 50% under three operating conditions is 9940s, 9530s, and 8940s, respectively. When the operating condition is changed from horizontal up-in and down-out to horizontal down-in and up-out, or vertical up-in and up-out, the time required for 50% of the PCM in the device to melt is shortened by 4.12% and 10.06%, respectively. The time required for 90% of the PCM in the device to melt is 20710s, 20680s, and 17770s, respectively. When the operating condition is changed from horizontal up-in and down-out to horizontal down-in and up-out, or vertical up-in and up-out, the time required for 90% of the PCM in the device to melt is shortened by 0.14% and 14.20%, respectively. In conclusion, the heat storage performance of the device is significantly better in the vertical installation mode than in the horizontal installation mode, while the effect of changing the water inlet direction on the heat storage performance of the device is small in the horizontal installation mode. Additionally, the time required for the device's average temperature to reach 60℃ under the three operating conditions is 23720s, 23250s, and 19420s, respectively. When the operating condition is changed from horizontal up-in and down-out to horizontal down-in and up-out, or vertical up-in and up-out, the time required for the device average temperature to reach 60℃ is shortened by 1.98% and 18.13%, respectively. From the graph, it can be seen that within the first 4 hours of heat storage, the average temperatures of the device under the three operating conditions are similar, while after 4 hours, the vertical installation device has a significantly improved temperature rise rate.

Preprints (www.preprints.org) | NOT PEER-REVIEWED | Posted: 18 April 2023 doi:10.20944/preprints202304.0481.v1

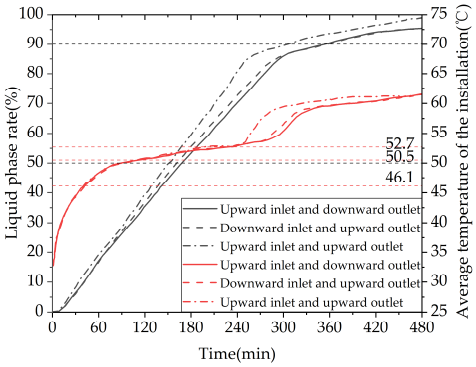

Figure 33. The liquid fraction and average temperature of the phase change heat storage unit vary with different inlet flow directions and installation orientations.

6. Conclusions

This article presents an experimental study on the factors affecting the performance of a phase change TES system. The following conclusions are drawn:

(1) Inlet temperature has a significant impact on TES performance. For the charging process, a higher inlet temperature leads to an earlier start time of TES, faster attainment of the charging termination temperature, and an increase in both the total and the average charging power. For the discharging process, a higher inlet temperature delays the start time of discharging slows down the attainment of the discharging termination temperature, and prolongs the effective discharging time. However, this also reduces the effective discharging energy of in the system.

(2) Inlet flow rate has a certain impact on TES performance, but the improvement is limited. For the charging process, a higher inlet flow rate leads to faster attainment of the charging termination temperature, but the difference is not significant. Increasing the inlet flow rate can reduce the temperature difference between the inlet and outlet, thus improving the charging performance, but it also reduces the charging power. For the discharging process, a higher inlet flow rate leads to faster attainment of the discharging termination temperature and can improve the effective discharging energy and efficiency, as well as prolong the effective discharging time. However, the improvement is relatively limited.

(3) Changing the type of heat storage has a certain impact on the TES performance. Adding an electric heating plate to assist in the heating of the water can significantly accelerate the melting process of the phase change material and improve the charging power.

(4) Increasing the initial temperature of the TES can prolong the effective discharging time, improve the discharging performance, and significantly increase the sensible heat discharge power. However, when the temperature is increased beyond a certain point, the improvement effect gradually diminishes.

In addition, numerical simulation is conducted to optimize the structure and operating conditions of the TES system, and the following conclusions are drawn:

(1) The staggered placement of fins is slightly better than the aligned placement, but the difference is not significant.

(2) Reducing the fin spacing and increasing the fin thickness can improve the melting efficiency of the phase change material and shorten the TES time.

(3) The TES performance of the vertically installed system is significantly better than that of the horizontally installed system, and the difference is mainly reflected in the later stage of the TES. When the system is horizontally installed, the down-inlet and up-outlet heat exchange mode has slightly better charging performance than the up-inlet and down-outlet mode, and the difference is mainly reflected in the early stage of the TES.

Author Contributions: Methodology, software, investigation, and writing—original draft preparation, Yuqing Tang; conceptualization, resources, supervision, project administration, and funding acquisition, Neng Zhu;

validation, formal analysis, data curation, and visualization, Siqi Li; writing—review and editing, Yingzhen Hou. All authors have read and agreed to the published version of the manuscript. Please turn to the CRediT taxonomy for the term explanation. Authorship must be limited to those who have contributed substantially to the work reported.

Funding: This research received no external funding

Data Availability Statement: The manuscript included all required data and implementing information.

Conflicts of Interest: The authors declare no conflict of interest.

References:

1. Xiao, J.H., Exploring the technology of solar energy application in buildings. *Scientific and Technological Innovation* **2019**, (25), 107-108.
2. Ke, L.; Fanneng, H., Analysis on Mainland China's Solar Energy Distribution and Potential to Utilize Solar Energy as an Alternative Energy Source. *Progress in Geography* **2010**, 32, 1672-1678.
3. Prieto, M.M.; Suárez, I.; González, B., Analysis of the thermal performance of flat plate PCM heat exchangers for heating systems. *Appl Therm Eng* **2017**, 116, 11-23.
4. ElGhnam, R.I.; Abdelaziz, R.A.; Sakr, M.H.; Abdelrhman, H.E., An experimental study of freezing and melting of water inside spherical capsules used in thermal energy storage systems. *Ain Shams Eng J* **2012**, 3, (1), 33-48.
5. Shamsi, H.; Boroushaki, M.; Geraei, H., Performance evaluation and optimization of encapsulated cascade PCM thermal storage. *J Energy Storage* **2017**, 11, 64-75.
6. Agyenim, F.; Hewitt, N.; Eames, P.; Smyth, M., A review of materials, heat transfer and phase change problem formulation for latent heat thermal energy storage systems (LHTESS). *Renewable and Sustainable Energy Reviews* **2010**, 14, (2), 615-628.
7. Vyshak, N.R.; Jilani, G., Numerical analysis of latent heat thermal energy storage system. *Energ Convers Manage* **2007**, 48, (7), 2161-2168.
8. Seban, R.A.; McLaughlin, E.F., Heat transfer in tube coils with laminar and turbulent flow. *Int J Heat Mass Tran* **1963**, 6, (5), 387-395.
9. Liang, H.; Niu, J.; Gan, Y., Performance optimization for shell-and-tube PCM thermal energy storage. *J Energy Storage* **2020**, 30.
10. Tay, N.H.S.; Bruno, F.; Belusko, M., Comparison of pinned and finned tubes in a phase change thermal energy storage system using CFD. *Appl Energ* **2013**, 104, 79-86.
11. Rathod, M.K.; Banerjee, J., Thermal performance enhancement of shell and tube Latent Heat Storage Unit using longitudinal fins. *Appl Therm Eng* **2015**, 75, 1084-1092.
12. Mat, S.; Al-Abidi, A.A.; Sopian, K.; Sulaiman, M.Y.; Mohammad, A.T., Enhance heat transfer for PCM melting in triplex tube with internal-external fins. *Energ Convers Manage* **2013**, 74, 223-236.
13. Al-Abidi, A.A.; Mat, S.; Sopian, K.; Sulaiman, M.Y.; Mohammad, A.T., Internal and external fin heat transfer enhancement technique for latent heat thermal energy storage in triplex tube heat exchangers. *Appl Therm Eng* **2013**, 53, (1), 147-156.
14. Pei, Y.; Yaping, H.; Jianjun, W.; Yanli, L., Numerical Simulation on Solid-liquid Phase Change Process of Thermal Storage Equipment with Inner Fins. *Journal of North China University of Water Resources and Electric Power (Natural Science Edition)* **2016**, 37, (03), 89-92.
15. Castell, A.; Sole, C.; Medrano, M.; Roca, J.; Cabeza, L.F.; Garcia, D., Natural convection heat transfer coefficients in phase change materia (PCM) modules with external vertical fins. *Appl Therm Eng* **2008**, 28, (13), 1676-1686.
16. Shatikian, V.; Ziskind, G.; Letan, R., Numerical investigation of a PCM-based heat sink with internal fins. *Int J Heat Mass Tran* **2005**, 48, (17), 3689-3706.
17. Campos-Celador, A.; Diarce, G.; Teres Zubiaga, J.; Bandos, T.V.; Garcia-Romero, A.M.; Lopez, L.M.; Sala, J.M., Design of a finned plate latent heat thermal energy storage system for domestic applications. In *Proceedings of the 2nd International Conference on Solar Heating and Cooling for Buildings and Industry (SHC 2013)*, Haberle, A., Ed 2nd International Conference on Solar Heating and Cooling for Buildings and Industry (SHC), **2014**; Vol. 48, pp 300-308.
18. Prieto, M.M.; Gonzalez, B.; Granado, E., Thermal performance of a heating system working with a PCM plate heat exchanger and comparison with a water tank. *Energy Buildings* **2016**, 122, 89-97.

19. N. K. BANSAL, D.B., An Analytical Study of a Latent Heat Storage System in a Cylinder. *Energy Conversion & Management* **1992**, 33, (4), 235-242.
20. Rathod, M.K.; Kanzaria, H.V., A methodological concept for phase change material selection based on multiple criteria decision analysis with and without fuzzy environment. *Materials & Design* **2011**, 32, (6), 3578-3585.
21. Xu, H.; Sze, J.Y.; Romagnoli, A.; Py, X., Selection of Phase Change Material for Thermal Energy Storage in Solar Air Conditioning Systems - Science. Energy Procedia **2017**,105,4281-4288.
22. Al-Abidi, A.A.; Mat, S.; Sopian, K.; Sulaiman, M.Y.; Mohammad, A.T., Experimental study of PCM melting in triplex tube thermal energy storage for liquid desiccant air conditioning system. *Energy and Buildings* **2013**, 60, 270-279.
23. Hosseini, M.J.; Ranjbar, A.A.; Sedighi, K.; Rahimi, M., A combined experimental and computational study on the melting behavior of a medium temperature phase change storage material inside shell and tube heat exchanger. *International Conference in Heat and Mass Transfer* **2012**, 39, (9), 1416-1424.
24. Rathod, M.K.; Banerjee, J., Experimental Investigations of Latent Heat Storage Unit Using Paraffin Wax as PCM. *Experimental Heat Transfer* **2014**, 27, (1), 40-55.
25. Le-li, W.; Ye, W.; Wei-wei, W.; Liang-bi, W., Fully Coupled Numerical Analysis on Thermal Storage Performance of Shell and Tube Bundle Latent Heat Thermal Storage. *Journal of Lanzhou Jiaotong University* **2019**, 38, (04), 65-74.